



الجمهورية الجزائرية الديمقراطية الشعبية
République Algérienne Démocratique et Populaire
وزارة التعليم العالي والبحث العلمي
Ministère de l'Enseignement Supérieure et de la Recherche Scientifique

جامعة وهران 2 محمد بن أحمد
Université d'Oran 2 Mohamed Ben Ahmed
معهد الصيانة و الأمن الصناعي
Institut de Maintenance et de Sécurité Industrielle

Département: Maintenance en Électromécanique

MÉMOIRE

Pour l'obtention du diplôme de Master

Filière: Électromécanique

Spécialité : Maintenance en Électromécanique industrielle

Thème

CFD Simulation of Gas Turbine

Blade Cooling

Présenté par:

BADJOUDA ZAKARIA

et

KHARCHOUCHE OTHMAN

ABDALLAH

Devant le jury composé de :

NOM ET PRÉNOM	Grade	Établissement	Qualité
NOUREDDINE RACHID	PR	IMSI-Université d'Oran 2	Président
DARRAMDANE MOHAMED ZOUHIR	MCB	IMSI-Université d'Oran 2	Encadreur
ACHACHE HABIB	MCA	IMSI-Université d'Oran 2	Examinateur

Année 2021/2022



الجمهورية الجزائرية الديمقراطية الشعبية
République Algérienne Démocratique et Populaire
وزارة التعليم العالي والبحث العلمي
Ministère de l'Enseignement Supérieure et de la Recherche Scientifique

جامعة وهران 2 محمد بن أحمد
Université d'Oran 2 Mohamed Ben Ahmed

معهد الصيانة و الأمن الصناعي
Institut de Maintenance et de Sécurité Industrielle

Department: Maintenance in Electro-mechanics

MEMORY

For obtaining the Master's degree

Sector: Electro-mechanics

Specialty: Maintenance in Industrial Electro-mechanics

Theme

**CFD Simulation of Gas Turbine
Blade Cooling**

Presented by:

BADJOUDA ZAKARIA

AND

KHARCHOUCHE OTHMAN

ABDALLAH

In front of the jury composed of:

FULL NAME	Grade	Establishment	Quality
NOUREDDINE RACHID	PR	IMSI-University of Oran 2	President
DARRAMDANE MOHAMED ZOUHIR	MCB	IMSI-University of Oran 2	Framer
ACHACHE HABIB	MCA	IMSI-University of Oran 2	Examiner

Year 2021/2022

Thanks

This work is the culmination of hard work and many sacrifices. First of all, we thank the almighty who, by his grace, allowed us to reach the end of our efforts by giving us health, strength, courage and by having us surrounded by wonderful people whom we would like to thank.

We would like to express our thanks to our families who have always supported and pushed us to continue and to go ahead until the end.

We would like to thank Mr DARRAMDANE Mohamed Zouhir, our teacher and supervisor. His support, skills, and foresight were invaluable. We especially thank him for his attention, his advice, his patience, his availability and all the time he devoted to us in order to accomplish our work.

We express our gratitude to the president of the jury for agreeing to examine this dissertation. We would like to thank the members of the jury for having accepted to take part in this jury as well as for the interest they have shown in this work.

Thanks to all those who directly or indirectly contributed to the accomplishment of this work.

Dedications

I dedicate this work to my family, my mother and my brothers and sisters, whom where always there to have my back and support my steps, fix my slips and cover my flaws, without them I would have never been close to achieve any of this, they are the ones who made me the person I am today, and for that I will always be grateful to them, for I can never repay a tiny bit of their kindness.

To my friends and colleagues whom shared this journey with me all the way through from the beginning to the end, Abdelmalek, Younes and Mohamed.

To my bros,

Rachid, Nouredine and Toufik.

And finally to my partner Zaki, and all Badjouda family.

ABDALLAH

Dedications

TO MY BELOVED FAMILY

I dedicate this work to my loved parents who have always teach me to trust in Allah, whose prays day and night make me able to get such success and honor also to my brothers and sister, whom believe in me support me and to all Badjouda's family, and Allane's family.

TO MY RESPECTED TEACHERS

Teachers are always great source of inspiration and motivation to me. However, their sincere guidance and prudent leadership guided my way clearly not only to excel in achieving this work but also definite directions for professional career too.

TO MY DEAR FRIENDS

My friends who stood with me, I would not be able to achieve my target without them easily. I'm more than thankful to all for their support and encouragement during the time.

Also dedication to my partner abdallah and his family.

ZAKARIA

Abstract

In this work, the numerical simulation of film cooling has been carried out using Ansys software.

Film cooling technique relies on injection of coolant fluid through internal channels manufactured in blade body in order to cool down turbine blade exposed to very high temperatures to prevent the damages in blade especially at the edges. This method is the most common in the cooling of gas turbine blades where the coolant fluid is injected inside the blade and moves outside through holes to protect the external surface. In this work three cases have been studied. The first case which represents the reference case a solid blade with no cooling method is presented. In the second case, three longitudinal channels are designed inside the blade to carry the cooling air through the body. In the third case additional holes are added to the main channels to load the cooling air into the outside surface of the blade creating a protection film around it.

Surface blade temperature is studied and it is clearly shown that the third case gives the optimum cooling performance where the cooling efficiency reached 79.8% and the temperature decreased by 55.43%.

المخلص

في هذا العمل ، تم تنفيذ المحاكاة العددية لتبريد الغشاء باستخدام برنامج ANSYS.

تعتمد تقنية تبريد الغشاء على حقن سائل التبريد من خلال القنوات الداخلية المصنوعة داخل جسم الشفرة من أجل تبريد ريش التوربين المعرضة لدرجات حرارة عالية جداً لمنع الأضرار في الشفرة خاصة عند الحواف. هذه الطريقة هي الأكثر شيوعاً في تبريد ريش التوربينات الغازية حيث يتم حقن سائل التبريد داخل الشفرة و يسري للخارج من خلال فتحات لحماية السطح الخارجي. في هذا العمل تمت دراسة ثلاثة حالات. يتم تقديم الحالة الأولى التي تمثل الحالة المرجعية وهي شفرة صلبة بدون طريقة تبريد. في الحالة الثانية ، تم تصميم ثلاث قنوات طويلة داخل الشفرة لنقل هواء التبريد عبر الجسم. في الحالة الثالثة، يتم إضافة ثقوب إضافية إلى القنوات الرئيسية لتحميل هواء التبريد إلى السطح الخارجي للشفرة مما يخلق طبقة حماية حولها.

تمت دراسة درجة حرارة النصل السطحي وتبين بوضوح أن الحالة الثالثة تعطي أداء تبريد مثالي حيث وصلت كفاءة التبريد إلى 79.8% وانخفضت درجة الحرارة بنسبة 55.43%.

Contents list :

<i>General introduction</i>	01
Chapter I : work carried out in film cooling	
<i>I.1 Introduction</i>	03
<i>I.2 Literature Review</i>	03
<i>I.3 Conclusion</i>	07
Chapter II: Operating principle and theoretical study	
<i>II.1 Introduction</i>	08
<i>II.2 Definition of gas turbine</i>	08
<i>II.3. Main elements of gas turbine</i>	08
<i>II.3.1 The compressor</i>	08
<i>II.3.2 The combustion chamber</i>	09
<i>II.3.3 The turbine</i>	09
<i>II.4 Operation principle of the gas turbine</i>	10
<i>II.5 Turbine blade cooling</i>	11
<i>II.5.1 Internal blade cooling</i>	12
<i>II.5.1.1 Convection cooling</i>	12
<i>II.5.2 External cooling</i>	13
<i>II.5.2.1 Film cooling</i>	13
<i>II.6 Coolant passages</i>	14
<i>II.6.1 Single pass</i>	14
<i>II.6.2 Multi-pass</i>	14
<i>II.7 Heat transfer</i>	15
<i>II.7.1 Conduction</i>	15
<i>II.7.2 Convection</i>	16
<i>II.7.3 Radiation</i>	16
<i>II.8 Film effectiveness</i>	16
<i>II.9 Blowing ratio</i>	17
<i>II.10 CFD software</i>	17
<i>II.11 Ansys CFX</i>	17
<i>II.11.1 Ansys ICEM</i>	18
<i>II.11.2 CFX-PRE</i>	19

II.11.3 CFX-solver	21
II.11.4 CFX-post	21
II.12 Solidworks	22
II.13 Finite volumes method	23
II.14 conclusion	23
Chapter III: Study of a case	
III.1 Introduction	26
III.2 Gas turbine blade modelling	26
III.3 Mesh generation	31
III.3.1 Mesh study	37
III.4 Pre processing	38
III.4.1 Domains inputs	38
III.4.2 Boundary condition	39
III.4.3 Interfaces	39
III.4.4 Solver control	41
III.5 CFX-POST	41
III.6 Conclusion	41
Chapter IV: Results and discussion	
IV.1 Introduction	40
IV.2 Results analyses of temperature and heat flux distribution	40
IV.2.1 Case 1	40
IV.2.2 Case 2	42
IV.2.3 Case 3	43
IV.3 Results analyses of effectiveness	47
IV.4 Conclusion	50
General conclusion	51

Nomenclature:

Φ : Heat flux transmitted (W).

λ : Thermal conductivity of the medium (W/m. °C).

X : Space variable in Flow direction (m).

S : Cross-sectional area of heat flux passage (m).

h : Coefficient of heat transfer by convection (W/ m. °C).

S : Surface area (m²).

T_c : Coolant temperature at the exit of the hole.(K)

T_∞ : Mainstream temperature (K).

T_p : Surface temperature (K).

σ : Stefan Boltzmann constant ($5.67 \cdot 10^{-8}$ W m K).

ϵ_p : Surface emission factor.

η : Cooling film effectiveness.

\vec{V}, \vec{U} : Velocity vector.

∇p : Pressure gradient.

ρ : Density of the fluid.

M : Blowing ratio.

Figures list :

<i>Fig I.1: Different cooling holes shapes made by Daniel G Hyams</i>	04
<i>Fig II.1: a compressor scheme</i>	09
<i>Fig II.2: A diagram of a gas turbine engine</i>	09
<i>Fig II.3: Pressure and temperature variations in the different sections of gas turbine</i>	10
<i>Fig II.4: Cooling flow in a turbine blade.</i>	12
<i>Fig II.5: Blade cooling by convection.</i>	12
<i>Fig II.6: Schematic of film cooling configurations on a vane</i>	13
<i>Fig II.7: Single pass blade cooling</i>	14
<i>Fig II.8: Multi-pass blade cooling</i>	15
<i>Fig II.9: Ansys CFX 2019</i>	18
<i>Fig II.10: Ansys ICEM 2019 interface</i>	19
<i>Fig II.11: Ansys CFX-Pre interface</i>	20
<i>Fig II.12: Ansys CFD-POST interface</i>	21
<i>Fig II.13: Process scheme of the simulation</i>	22
<i>Fig III.1: Blade airfoil-Solidworks</i>	24
<i>Fig III.2: Case (1) geometry design</i>	25
<i>Fig III.3: Case (2) geometry design</i>	26
<i>Fig III.4: Case (3) geometry design</i>	26
<i>Fig III.5: Hot domain geometry design.</i>	27
<i>Fig III.6: Vertices to points association</i>	29
<i>Fig III.7: Edges to curves association</i>	29
<i>Fig III.8: Blocking of case (1)</i>	30
<i>Fig III.9: Meshed domains for case (1)</i>	30
<i>Fig III.10: Blocking of case (2)</i>	31
<i>Fig III.11: Meshed domains for case (2)</i>	32
<i>Fig III.12: Tube hexahedral mesh</i>	33
<i>Fig III.13: Meshed domains for case (3)</i>	33
<i>Fig III.14: Mesh refinement at leading edge (view1)</i>	34
<i>Fig III.15: Mesh refinement at leading edge (view2)</i>	35
<i>Fig III.16: The pressure graphs given by the different meshes.</i>	36
<i>Fig III.17: Case (1) Pre-processing</i>	38

<i>Fig III.18: Case (2) Pre-processing</i>	38
<i>Fig III.19: Case (3) Pre-processing</i>	39
<i>Fig IV.1: Contour of temperature for blade surface case (1)</i>	41
<i>Fig IV.2: Contour of heat flux for blade surface case (1)</i>	41
<i>Fig IV.3: Contour of temperature for blade surface case 2</i>	42
<i>Fig IV.4: Contour of heat flux for blade surface case (2)</i>	43
<i>Fig IV.5: Contour of temperature for blade surface case (3)</i>	44
<i>Fig IV.6: Contour of heat flux for blade surface case (3)</i>	44
<i>Fig IV.7: Temperature distribution at intrados polyline for the three cases</i>	45
<i>Fig IV.8: Temperature distribution at extrados polyline for the three cases</i>	46
<i>Fig IV.9: Coolant temperature streamlines</i>	47
<i>Fig IV.10: Cooling effectiveness η distribution for case (2)</i>	48
<i>Fig IV.11: Cooling effectiveness η distribution for case (3)</i>	48
<i>Fig IV.12: Cooling effectiveness η variation at intrados polyline for case 2 and 3</i>	49
<i>Fig IV.13: Cooling effectiveness η variation at extrados polyline for case 2 and 3</i>	50

Tables List :

- Table III.1** *Airfoil design parameters*
- Table III.2** *film cooling holes configuration*
- Table III.3** *mechanical properties of Stainless steel*
- Table III.4** *Case 1 Mesh Details*
- Table III.5** *Case 2 Mesh Details*
- Table III.6** *Case 3 Mesh Details*
- Table III.7** *Mesh study details*
- Table III.8** *Boundary conditions input*

General introduction

General introduction:

In order to realize more power and further increase to the thermal efficiency of the modern gas turbine, it is essential to increase the inlet temperature of the turbine which is in a continuous increase by about 20°C per year and can reach about 1,700°C for a modern gas turbine.

Progress has been made possible in particular thanks to research efforts in the field of materials and alloys more resistant to high temperatures. Thus, the operating temperature of the blades has increased from 1080°C to 1180°C. Along with these improvements, cooling techniques were introduced and evolved into more comprehensive and complex systems. From a solid and non-cooled blade, we have seen the successive appearance of forced internal convection systems, air film protection devices, or even surface treatment methods acting as a thermal barrier.

Air film cooling is the most commonly used technique in the industry. In such a situation, cold air is supplied from the compressor to the turbine blades. Cold air is ejected through rows of holes in the waterfall passage and forms a protective film around the blade. The major aim of film cooling is to reduce the flow of cooling air while maintaining minimal aerodynamic losses with high thermal protection.

The objective of this work is to contribute to the understanding of complex phenomena that accompany film cooling.

Our choice of geometric is based on the study of the film cooling technique and the enhancement of the blades and turbine cooling efficiency.

The first chapter of this study is devoted to the literature review of the work carried out in the enhancement of film cooling of the turbine blades by different engineers in the field.

The second chapter of this study treats the operating principles and the theoretical study relating to the cooling of turbine blades. Thus, an exhaustive description of the different methods of cooling encountered in the industrial world is presented, followed by an overview of the different correlations used in the theoretical study of film cooling. Finally, this chapter is closed with a presentation of the CFD software used in the simulation, and a couple of equations related to the software calculations.

As for the third chapter, we presented the creation of the blades geometries using solidworks software, and the meshing of these geometries in the ansys ICEM software.

And the fourth and last chapter is devoted to the discussion of the simulation results obtained.

Chapter I:
Literature review

I.1 Introduction:

In order to obtain higher power output from the gas turbine engines, the turbine inlet temperature had been increased in the recent engines. This high temperature could lead to overheating of the blades and may result in blade failure and lead as well to engine failure and catastrophic effects. In order to prevent such failures, the blade surfaces must be maintained to acceptable limits of temperature. So, the cooling of blade surfaces must be considered. There are multiple cooling techniques such as convective cooling, impingement cooling etc. to maintain the surface temperature to an acceptable range. Film cooling is one such cooling process. In film cooling, the surface will be covered with a thin film of cool air that acts as a buffer between the high temperature gas and the surface. The cold air will be injected at high pressures through the holes in the surface, resulting in a thin cold film surrounding the hot surfaces. [1]

I.2 Literature Review:

Based on the surface concentration of a coolant such as Ammonia gas, **S.Friedrichs**[2] had developed a method to estimate the film cooling effectiveness. In his experiments, a thin film of 0.05 mm thickness of diazo surface coating was applied over the turbine cascades. Their cascade model consisted of four blades with a chord of 278 mm, span of 300 mm with the flow entering at 40°. The authors had compared the results against an experimental work conducted using a temperature based measurement techniques for film cooling. The results were in agreement apart from the regions near the coolant holes.

Daniel G Hyams[3] had studied the film cooling for the critical parameters such as blowing ratio (1.25, 1.88), Density ratio (1.6) and length to diameter ratio (4). His study included the experimental as well as CFD simulations. The authors had performed steady state, three dimensional simulations using RANS approach. They had studied five film cooling hole geometries: Cylindrical film hole, forward diffused film hole, laterally diffused film hole, inlet shaped film hole and cusp-shaped film holes. (fig I.1) Based on their results, the authors had observed that the film cooling shape had a significant impact on flow distributions at the exit plane which could further influence the downstream film cooling performances. Among the five film cooling holes studied in this work, the authors noted that the laterally diffused film holes provide better effectiveness. This could be attributed to the presence of weak longitudinal vortices which ensures the coolant films to firmly attach to the surface.

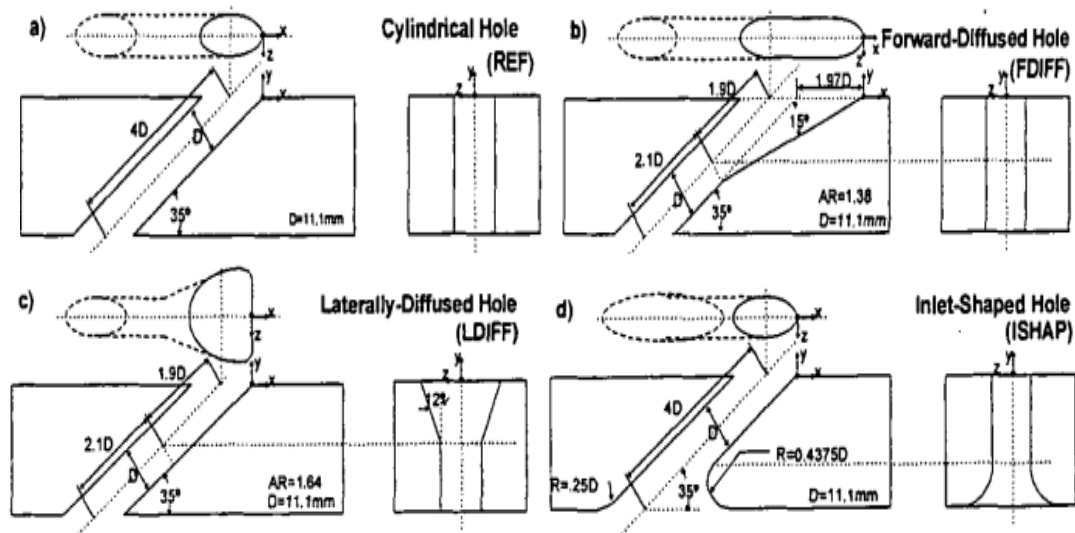


Fig I.1: different cooling holes shapes made by Daniel G Hyams[3]

The film cooling effectiveness and the resulting heat transfer coefficient on a cylindrical leading edge was studied experimentally with the help of a low-speed wind tunnel, corresponding to the flow conditions of $Re = 100,900$, by **Srinath V Ekkad**[4]. The injection holes on the cylindrical specimen were arranged in rows at $\pm 15^\circ$ from the stagnation. Their study focused on obtaining the film cooling effectiveness using liquid crystal technique. With the liquid crystal coatings on the cylinder surfaces, experiments were conducted to estimate the heat transfer coefficient and film cooling effectiveness. The cylindrical specimen was placed inside a tunnel with a cross section of 25.4 cm X 76.2 cm. A suction type blower was used for supplying air which is heated by the heater. The cylinder surface was also heated by a set of six cartridge heaters. Based on their findings, the authors had concluded that the Nusselt numbers, hence the heat transfer rate, increases with the increase in blowing ratio.

K. T. McGovern [5] had conducted computational along with experimental investigations for studying flow mechanisms for the film cooling for various compound injection angles (45° , 60° and 90°). Their computational studies were conducted using ANSYSFLUENT. In order to limit the numerical viscosity in the CFD simulations, the higher-order linear reconstructive discretization scheme was selected by the authors in their simulations. They had used the Reynolds Averaged Navier Stokes (RANS) approach, with standard k-epsilon for turbulence closure, in their investigations. The authors had invoked symmetry approach in these simulations because of the geometrical and the expected flow field symmetry. The CFD simulations were observed to be in good agreement with the

experimental data. They had concluded that the compound-angle injection method provides the lateral spreading of vortices in the domain, a significant parameter in enhancing heat transfer rate.

The film cooling heat transfer rate and the associated aerodynamic losses were experimentally studied by **J.E. Sargison**[6]. The geometry considered by the authors was a flat plate with a converging slot hole, defined as console, for film cooling. The author had compared the film cooling effectiveness for four different holes – slot, console, fan shaped and cylindrical – for pitch ratios. The experiment studies were corresponding to the flow conditions of $Re = 144,000$. From their study, the authors had observed that the console shaped film cooling method induces lesser aerodynamic losses as compared to the remaining cases. The laterally averaged heat transfer coefficient was higher in console and slot film cooling methods over the cylindrical and fan shaped film cooling holes.

Dibbon K Walters [7] had applied computational methods for jet-in-a-cross flow situation to study the relevant flow physics of film cooling. The CFD simulation was carried out using an implicit, pressure correction solver with multi-grid. The authors had studied for two different film-hole length-to-diameter ratios and the flow conditions corresponding to three blowing ratios ranging from 0.5 to 2.0. From their studies, they had observed that the vorticity in the boundary layers within the film hole were primarily responsible for the secondary motion.

Younggi Moon [8] had investigated the impact of the angle variation [0 to 75 degrees] between the primary and auxiliary film cooling holes of an anti-vortex hole. The film cooling effectiveness for varying blowing ratio [0.25 to 2.0] along with the free-stream turbulence was considered in this study. For the CFD simulations, the RNG k-epsilon turbulence model was chosen by the authors. The flow inlet to the computational domain was modeled using the ‘velocity-inlet’ boundary conditions while the ‘pressure-outlet’ boundary condition was applied for modeling the flow outlet. The authors had also conducted grid independence study by performing the simulations with 655,000, 1,246,000, 2,344,000 and 3,455,000 cells. For the final simulations, the 2,344,000 mesh was considered. Based on the results, the authors concluded that the film cooling effectiveness was strongly affected by the angle between the primary and auxiliary cooling holes.

Guangchao Li [9] had investigated the coolant cross-flow direction over the film cooling effectiveness. Their studies were conducted using the ANSYS FLUENT CFD solver. The authors had used the two-equation Realizable k-epsilon turbulence model. The second-

order upwind difference scheme was chosen for interpolating the advection and diffusion at the cell faces. The authors had investigated the cross-flow impact on the flow and film cooling effectiveness. Based on their findings, they concluded that the coolant cross-flow directions significantly affect the flow profile.

Xueying Li [10] had investigated the film cooling for the distribution of injection hole for a turbine vane. The authors had conducted the experiments along with the numerical simulations. The CFD simulations were performed using the boundary conditions such as ‘mass-flow-inlet’, ‘pressure-outlet’ and ‘wall’ with the relevant flow conditions. Considering the low speed conditions, the incompressible solution approach had been considered with SIMPLE algorithm proving the linkage between the pressure and the velocity. The authors argue that the local blowing ratio of the end-wall film cooling increased with the local static pressure. Since the cooling jets at the high local blowing ratio tend to be sensitive to the supply pressure, the film cooling holes located near the high static pressure locations could achieve wide range of blowing ratios.

Xueying Li [11] had varied conducted experiment as well as numerical simulations to study the influence of the film cooling effectiveness by varying the number of cooling jet rows. They had considered single row film cooling, three combinations of two row film cooling and full coverage configuration with five row cooling arrangements in their study. The CFD simulation for this work followed the earlier work by the authors [10]. The experiments were conducted using PSP technique by using the light emitting characteristics of PSP while at excitation. This light emission is inversely proportional to the oxygen pressure.

Xing Yang [12] had conducted numerical simulations using ANSYS CFX film cooling with swirling motion of coolant. They had used the cylindrical, clover shaped and compound angle holes in their studies. The authors had applied the Reynolds Averaged Navier Stokes (RANS) approach in their simulations with SST k-omega turbulence model being employed. The blowing ratio for this study was in the range of 0.5 to 1.5. The swirling motion of coolant flow had strong influence over the film cooling effectiveness, even more so at the higher blowing ratio.

I.3 Conclusion:

In this chapter of literature review, the work carried out in film cooling technique by few researchers is presented, the influence of some important parameters such as the shape, the angle of the cooling holes, the number of cooling jet rows, the blowing ratio are shown. it is clear that these studied parameters have a huge impact on the effectiveness of the film cooling.

Chapter II:
Operating principle
and theoretical study

II.1 Introduction:

Our study concerned with enhancing the cooling of the gas turbine blades. In this chapter we present the working principle of gas turbines, the methods for cooling the blades along with the film cooling for which we are most interested. The commercial code Ansys-CFX used in the simulation is presented as well in this chapter.

II.2 Definition of gas turbine:

A turbine is a rotating device intended to use the internal energy of the fluid (water, steam, air, combustion gas), characterized by its kinetic energy, potential energy and enthalpy, into mechanical energy and torque which is transmitted by means of a shaft to drive an alternator, a pump, a compressor or any other rotary mechanical receiver.

The gas turbine can be considered both external or internal combustion engine from all points of view., It is a self-sufficient system that takes and compresses atmospheric air in its own compressor, increases the energetic power of the air in its combustion chamber and converts this power into useful mechanical energy during the expansion processes that take place in the turbine section. The resulting mechanical energy is transmitted through a coupling to a receiving machine, which produces the power useful for the industrial process. Compared to other thermal engines, the gas turbine has a particularity; as well as the steam turbine, it has a continuous flow machine, therefore does not involve periodic variations of the state of fluid, in all given sections.

The gas turbine, also called combustion turbine, is a heat engine that is currently very popular, given its excellent performance (efficiency greater than 35% used alone, and 55% in the combined cycle). In its simplest and most widespread form, this machine is made up of three elements.

II.3. Main elements of gas turbine:**II.3.1 The compressor:**

A compressor (figure II.1), generally centrifugal or axial, which is used to compress the ambient air to a pressure comprised in modern machines.

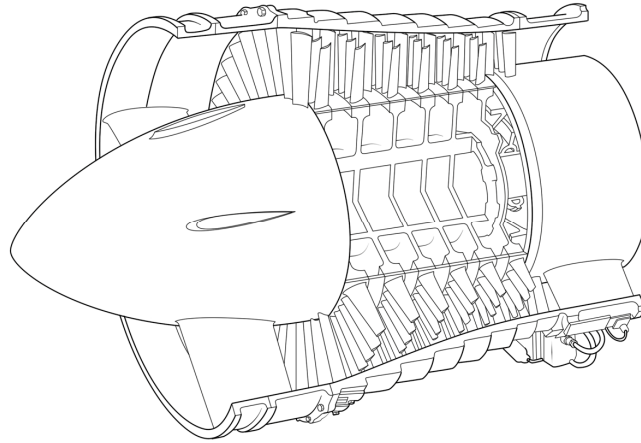


Fig II.1: a compressor scheme [13]

II.3.2 The combustion chamber:

A combustion chamber, in which fuel injected under pressure, is burned with previously compressed air.

II.3.3 The turbine:

In a gas turbine the high temperature gases leaving the combustion chamber are expanded. And the turbine supplies mechanical energy to the outside. A significant part (60 to 70%) of the work recovered on the turbine shaft is used to drive the compressor. The gas turbine function principle is shown in figure II.2.

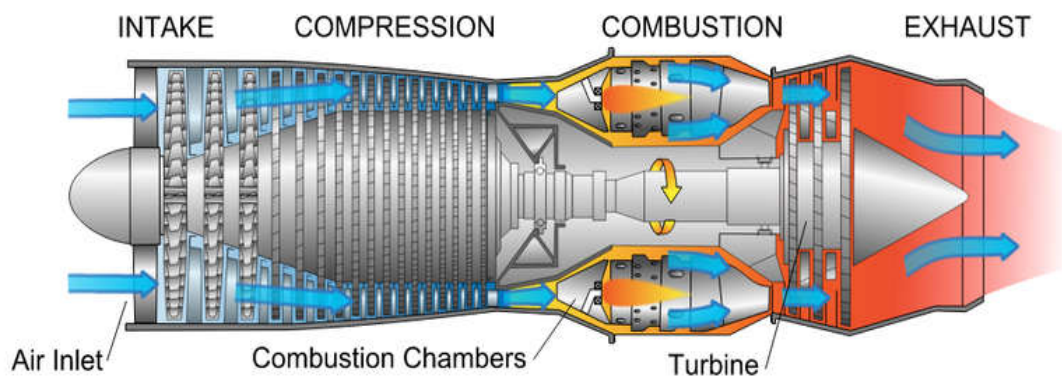


Fig II.2: A diagram of a gas turbine engine.[14]

II.4 Operation principle of the gas turbine:

A gas turbine works as follows:

- It extracts air from the surrounding environment.
- It compresses it to a higher pressure.
- It increases the energy level of compressed air by adding and burning fuel in a combustion chamber.
- it delivers air at high pressure and temperature to the turbine section, which converts thermal energy into mechanical energy to spin the shaft; this serves, on the one hand, to provide the useful energy to the driven machine, coupled with the machine by means of a coupling and, on the other hand, to provide the energy necessary for the compression of the air, which takes place in a compressor connected directly to the turbine section.
- It discharges to the atmosphere the gases at low pressure and temperature resulting from the transformation mentioned above.

Figure II.3 shows the pressure and temperature variations in the different sections of the machine corresponding to the operating phases mentioned above.

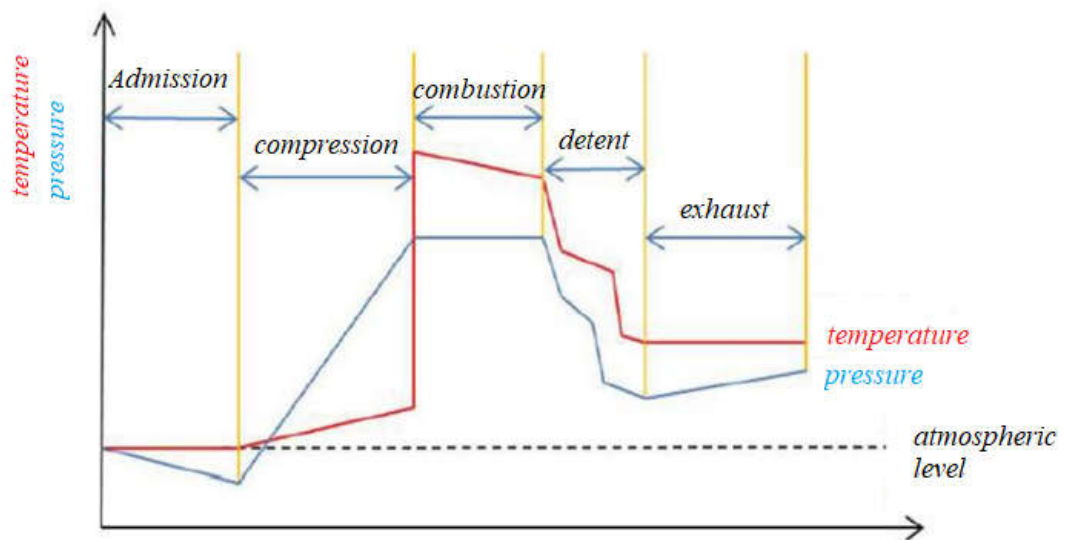


Fig II.3: pressure and temperature variations in the different sections of gas turbine.[15]

II.5 Turbine blade cooling:

The limitations of today's gas turbines are defined by the current cooling technologies as applied to the hot-section components. As a result of pursuing high operational efficiency the turbine inlet temperature is continuously prompted in the advancement of aero-engines. For the next generation of aero-engines, the turbine inlet gas temperature is expected to be beyond 2200 K, which is extremely higher than the limit operating temperature of most substrate materials without significant deterioration. Meanwhile, the coolant usage for the cooling purpose will be more limited. Thus, in the development of advanced aero-engines, the thermal protection of hot section components is one of the most critical challenges, without a doubt. [16]

At a constant pressure ratio, thermal efficiency of the engine increases as the turbine entry temperature increases. However, high temperatures can damage the turbine, as the blades are under large centrifugal stresses and materials are weaker at high temperature. So, turbine blade cooling is essential. [17] Current modern turbine designs are operating with inlet temperatures higher than 1900 Kelvin which is achieved by actively cooling the turbine components. [18]

Cooling of components can be achieved by air or liquid cooling. Liquid cooling seems to be more attractive because of high specific heat capacity and chances of evaporative cooling but there can be leakage, corrosion, choking and other problems, and this works against this method.[17] On the other hand, air cooling allows the discharged air into main flow without any problem. Quantity of air required for this purpose is 1–3% of main flow and blade temperature can be reduced by 200–300 °C.[17] There are many techniques of cooling used in gas turbine blades; convection, film, transpiration cooling, cooling effusion, pin fin cooling etc. which fall under the categories of internal and external cooling. While all methods have their differences, they all work by using cooler air (often bled from the compressor) to remove heat from the turbine blades. [19] Figure II.4 shows the cooling flow in a turbine blade and the passage it takes.

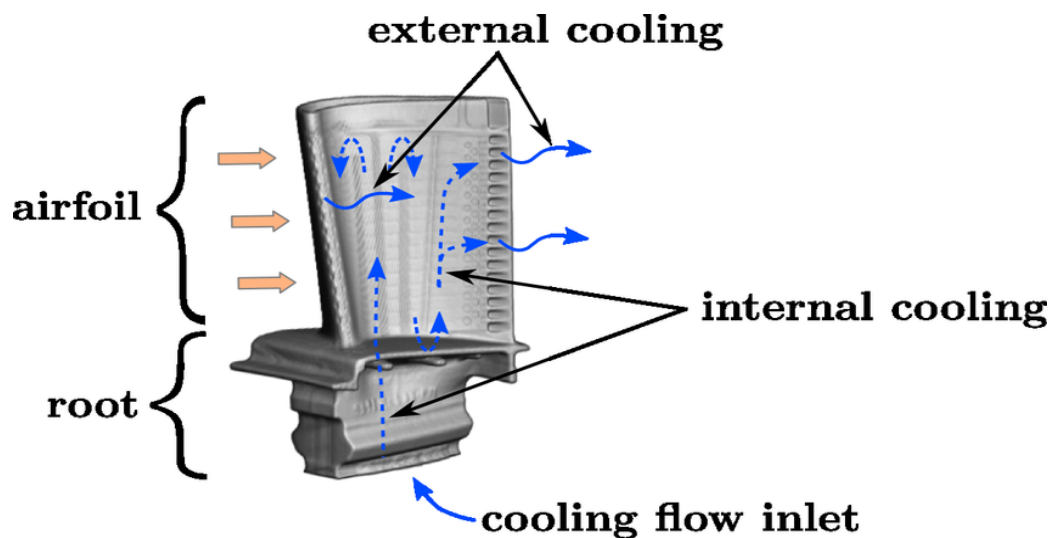


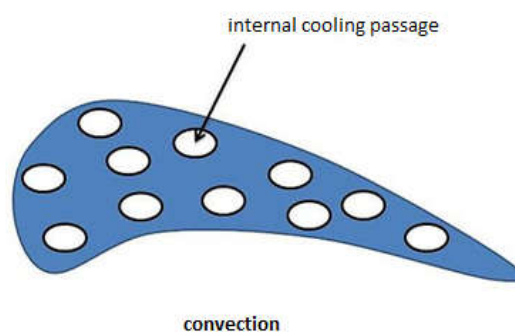
Fig II.4: Cooling flow in a turbine blade.[18]

II.5.1 Internal blade cooling:

II.5.1.1 Convection cooling:

Convection cooling works by passing cooling air through passages internal to the blade. Heat is transferred by conduction through the blade, and then by convection into the air flowing inside of the blade [19]. The internal passages in the blade may be circular or elliptical in shape. Cooling is achieved by passing the air through these passages from hub towards the blade tip. This cooling air comes from an air compressor [19].

The cooling fluid passes through the cooling passage and mixes with the hot main stream at the blade tip and the heat is exchanged by convection between the two fluids as shown in figure II.5.

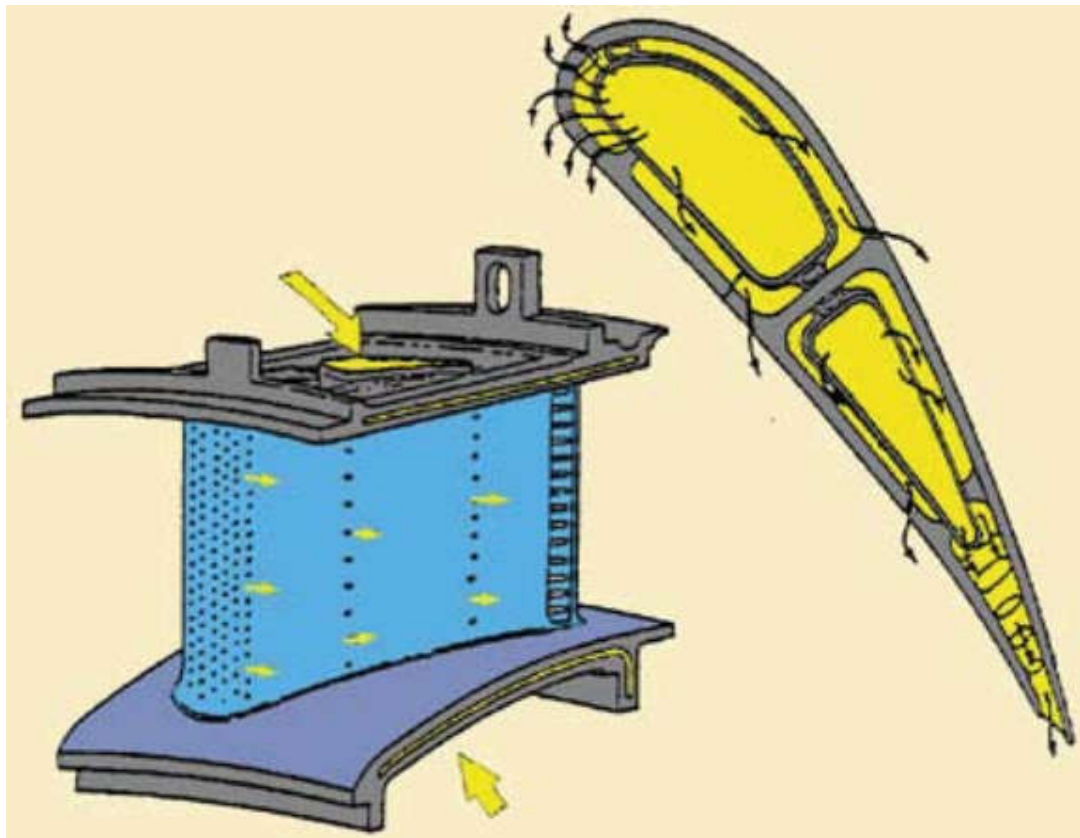


FigII.5: Blade cooling by convection.[20]

II.5.2 External cooling:

II.5.2.1 Film cooling:

Film cooling is a major component of the overall cooling of turbine airfoils. An example of a film cooled turbine vane is shown in figure II.6. From the schematic of the airfoil in figure II.6 there are holes placed in the body of the airfoil to allow coolant to pass from the internal cavity to the external surface. The ejection of coolant gas through holes in the airfoil body results in a layer or “film” of coolant gas flowing along the external surface of the airfoil. Hence the term “film cooling” is used to describe the cooling technique. Since this coolant gas is at a lower temperature than the mainstream, the heat transfer into the airfoil is reduced. [21]



FigII.6: Schematic of film cooling configurations on a vane [21]

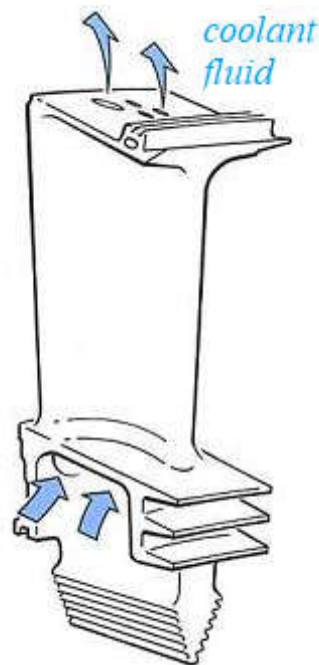
II.6 Coolant passages:

The passages the coolant takes while it is inside the airfoil varies from an old technique that can be summed under the name “single pass” to a newer one that is more complex and efficient which is “multi-pass”.

II.6.1 Single pass:

The early blades had a single pass so the air would come in at the blade route and it would have a short pass straight up through the blade and out through the holes that take place on the tip of the blade.

There are holes along the length of the blade as well where the cooling air can come out from.(figure II.7)

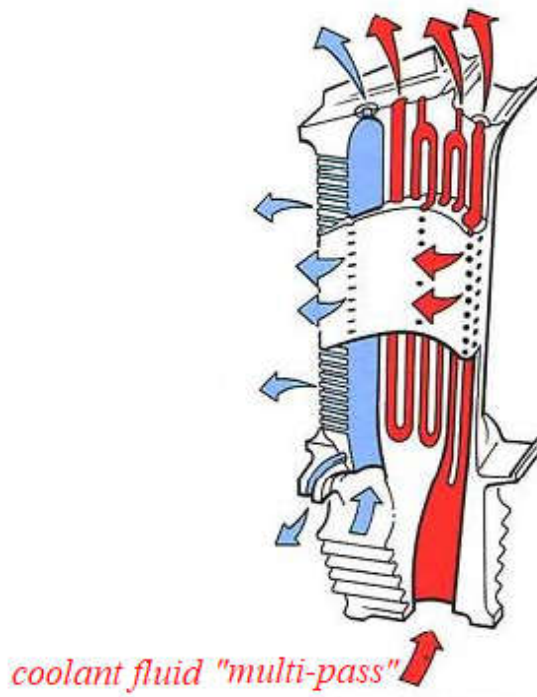


FigII.7: single pass blade cooling [22]

II.6.2 Multi-pass:

After “single pass” the cooling technique has evolved to the multi-pass, with the multi-pass the air comes in at the blade route and then takes a snake like pattern sometimes referred to as serpentine cooling and comes out through the tip, with holes

along that path, so the distance the air travels is greater which gives a greater cooling capability to the blade and increases the efficiency.(figure II.8)



FigII.8 : Multi-pass blade cooling [22]

II.7 Heat transfer review:

The basic requirement for heat transfer is the presence of a temperature difference. There is no net heat transfer between two mediums that are at the same temperature. The temperature difference is the driving force for heat transfer, just as the voltage difference is the driving force for electric current flow and pressure difference is the driving force for fluid flow. [23]

The main goal of heat transfer analysis is to study the temperature field. The gradient and time rate of change in temperature and the rate of flow of heat under steady state and transient conditions. In general there are three modes of heat transfer [24], conduction, convection and radiation.

II.7.1 Conduction:

It is the transfer of heat from hot parts to colder parts of the same body or two bodies in contact without apparent movement of matter.

Conduction theory relies on Fourier's assumption that flux density is proportional to temperature gradient:

$$\Phi = -\lambda S(\partial T/\partial X) \quad (\text{II.1})$$

This is called Fourier's law of heat conduction after J. Fourier, who expressed it first in his heat transfer text in 1822.

II.7.2 Convection:

The transfer of heat between a solid and a fluid, the energy being transmitted by displacement of the fluid, this transfer mechanism is governed by Newton's law:

$$\Phi = h s (T_p - T_\infty) \quad (\text{II.2})$$

II.7.3 Radiation:

It is a transfer of electromagnetic energy between two surfaces (even in vacuum). In conduction problems, we take into account the radiation between a solid and the surrounding medium and we have the relation:

$$\Phi = \epsilon \rho S (T_p^4 - T_\infty^4) \quad (\text{II.3})$$

II.8 Film effectiveness:

The primary process by which film cooling reduces the heat transfer to the wall is by reducing the gas temperature near the wall, i.e. reducing the driving temperature potential for heat transfer to the wall. As the coolant flows from the coolant holes, it mixes with the mainstream gas resulting in an increase in coolant temperature. [21]

The film effectiveness η is defined as follows:

$$\eta = \frac{T_\infty - T}{T_\infty - T_c} \quad (\text{II.4})$$

Where T is the local temperature, T_∞ is the mainstream temperature, and T_c is the coolant temperature at the exit of the hole.

Note that $\eta = 1$ is the normalized initial coolant temperature and $\eta = 0$ is the normalized mainstream temperature.

II.9 Blowing ratio:

Blowing ratio or Injection ratio “M”, is the ratio of the coolant mass flux to the mainstream mass flux and is defined as follows [21]:

$$M = \frac{\rho_c U_c}{\rho_\infty U_\infty} \quad (\text{II.5})$$

II.10 CFD Software:

CFD is an acronym of the English word Computational Fluid Dynamics, the word Computational refers to mathematics and calculations, and Fluid Dynamics to the branch of applied science that is concerned with the movement of liquids and gases. CFD software is therefore used to solve problems of flowing fluid dynamics. With this software we can build a model numerical of the studied system. Associated with the boundary conditions, its execution can provide us a prediction on the dynamics of the fluid and the physical phenomena generated.

There are three compelling reasons why the use of CFD codes is essential these days:

1. They allow a very good visualization of the flow especially in the case where one has a difficult system to build or to test experimentally. CFD software allows us to go inside the prototype created and see in detail the structure of the flow and the different physical phenomena generated.
2. This software makes it possible to test several designs under different operating conditions in order to achieve optimum operating results in a very short time. All of this can be done even before building the actual prototype.
3. Thanks to the results of the prediction, we obtain better designs, in very short times and in compliance with industrial and environmental regulations.

II.11 Ansys CFX:

In our simulations we are using Ansys-CFX 19.0; reliable computer software specialized in the fields of fluid mechanics and heat transfer. (figure II.9)

Ansys has several industrial applications. It is used to perform simulations ranging from the air flow around an airplane wing profile during combustion in the furnaces, bubble columns to the production of ice, from the flow of blood in the vessels to the manufacture of semiconductors, from room air-conditioning installations to wastewater treatment plants. The

software is able to model flows as complex as those in the cylinders of an internal combustion engine, in the turbo-machinery or in multiphase systems. This served to expand its range of use. In addition to its versatility, Ansys remains easy for users to master. Thanks to its simple and complete interface.

Typically Ansys users break down larger structures into small components that are each modeled and tested individually.

A user may start by defining the dimensions of an object and then adding weight, pressure, temperature and other physical properties.

Finally, the Ansys software simulates and analyzes movement, fatigue, fractures, fluid flow, temperature distribution, electromagnetic efficiency and other effects over time.

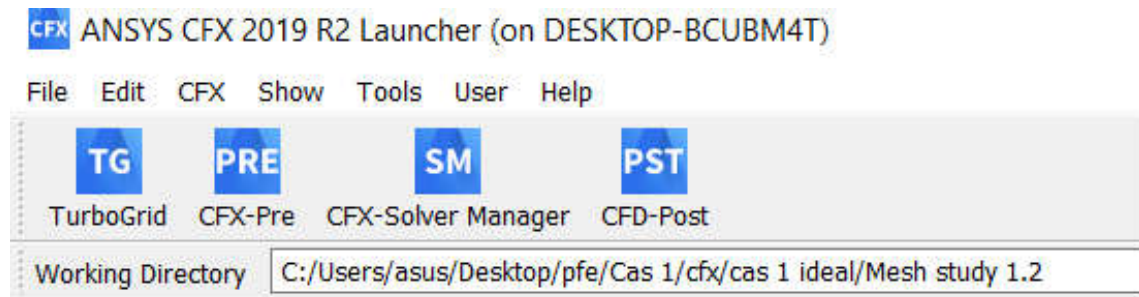


Fig II.9: Ansys CFX 2019

II.11.1 Ansys ICEM:

ANSYS ICEM CFD offers mesh generation with the capacity to compute meshes with various different structures depending on the user's requirements. It is powerful and highly manipulative software which allows the user to generate grids of high resolution.(figure II.10)

The ICEM CFD module makes it possible to establish the geometry of the system studied. It is used like traditional CAD software: geometry is constructed from points, curves, surfaces and volume. It is also this module which makes it possible to generate a mesh based on the geometry

The user then sets the mesh parameters he wishes to obtain on curves, surfaces and in volumes. The module allows generating tetrahedral, hexahedral and prismatic meshes. Once the mesh is done,

ICEM creates a file with the extension “.cfx5”, which groups the information relating to the mesh, exploitable by CFX-pre

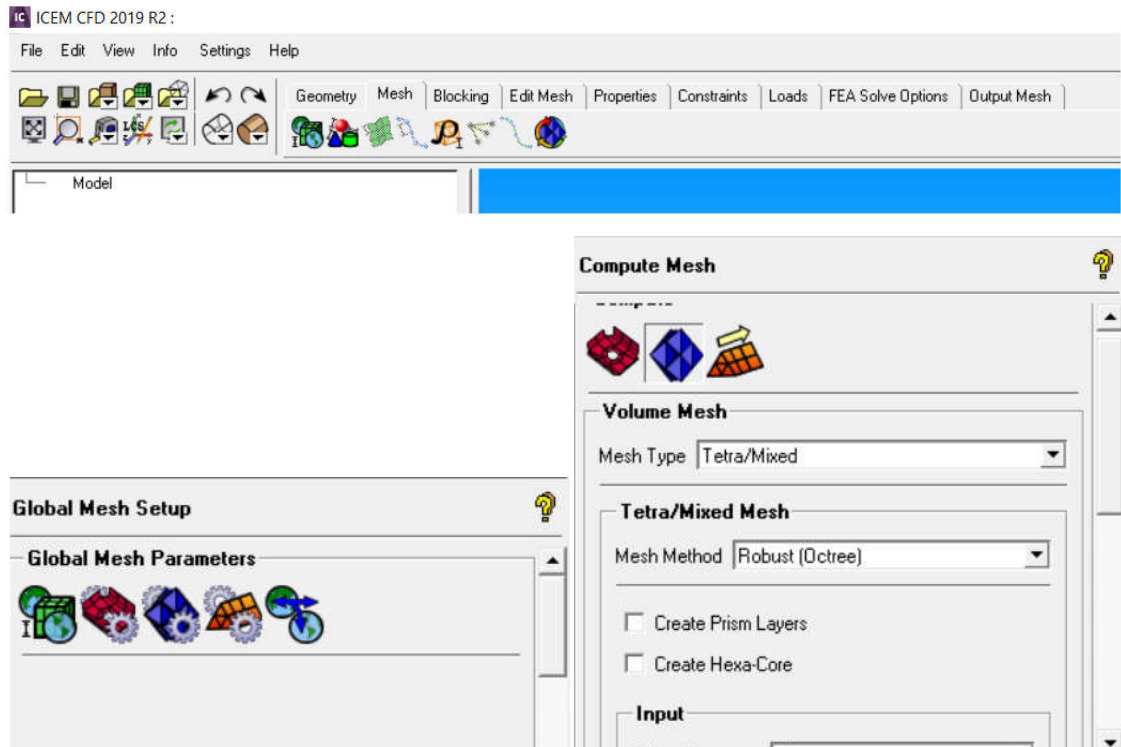


Fig II.10: Ansys ICEM 2019 interface

II.11.2 CFX-PRE:

CFX-Pre offers a modern, consistent and intuitive interface for defining complex CFD problems. CFX-Pre can read multiple meshes from a variety of sources.(figure II.11)

The user is guided through the physical definition by moving along the ‘Define’ toolbar, which presents the main steps in defining the problem.

The creation and modification of physical objects is presented through a user interface with tabbed panels providing easy access to model details. The evolving problem definition is shown in the ‘object selector’, which shows the main objects that can be chosen to access any stage of the problem definition. Errors that occur during problem definition or modification are shown using color coding in the object selector, or through descriptive messages in the physical message panel.

The CFX-pre module is used to define the boundary and initial conditions of the system, as well as the equations to be solved, the type of resolution (steady state or transient),

the solver parameters, including: the time step , the number of iterations, the convergence criterion as well as the nature of the fluids (or solids) present.

The boundary conditions are of 5 types: INLET, OUTLET, OPENING, WALL and SYMET.

- ❖ INLET type conditions are used in the case of a flow entering inside the domain
- ❖ The OUTLET type conditions are used in the case of an outgoing flow outside the domain.
- ❖ The OPENING condition is used in the case of a misunderstanding of the incoming or outgoing flow.
- ❖ The boundary condition of the WALL type is attributed to walls impermeable to flow.
- ❖ Finally, if the flow has a plane of symmetry, it is possible to assign the SYMMETRY condition to this plane

Once all the parameters have been defined, CFX-pre generates a ".def" file which contains all the information relating to the mesh, the boundary and initial conditions, as well as all the other parameters introduced in CFX-pre. It is this file that will be the work base of the solver.

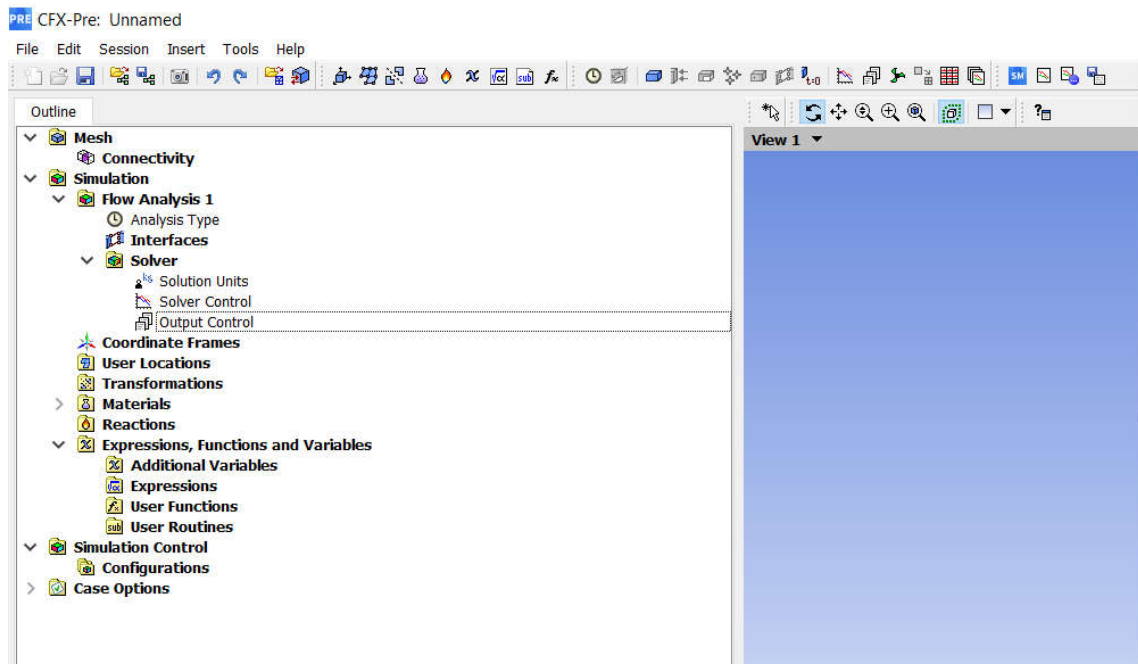


Fig II.11: Ansys CFX-Pre interface

II.11.3 CFX-solver:

The CFX-solve module is the module that performs the calculations. It is based on the integration of the NavierStokes equations in each mesh and has additional models to take into account turbulence, thermal radiation, etc. It provides a graphical interface to the CFX-Solver in order to provide information on the evolution of the solution. Its main functions are listed as follows:

- Indicate the input files to the CFX-Solver;
- Start or stop the simulation with CFX-Solver
- Modify some parameters in the definition file;
- Monitor the progress of the solution with CFX-Solver;
- Launch another simulation in parallel

At the end of its calculation, CFX-solve generate two types of files:

- An “.out” file readable by a text editor. This file summarizes the course of the calculation. It contains, among other things, the information of the "def" as well as the mass balance of the system.
- A ".res" file that contains all the results. This file is directly usable by CFX-post

II.11.4 CFX-post:

The CFX-post module is a graphical tool for processing and displaying results. It allows you to apply textures to the geometry, to visualize contours, iso surfaces, streamlines, velocity fields, etc. It also allows the export of results in digital form, such as the value of the different variables on each node, in photographic form and even in the form of animation.

Likewise, it allows you to export the results in different formats in order to process them on other graphics software.(figure II.12)

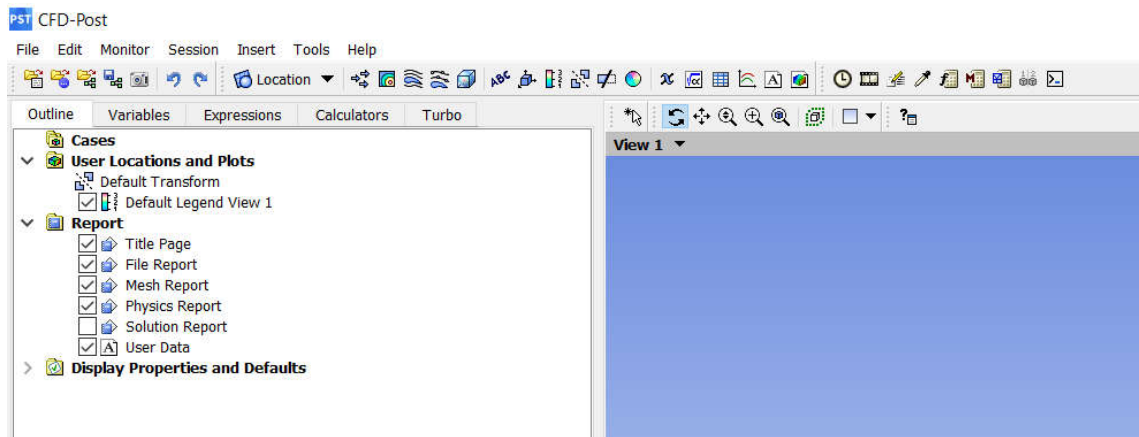


Fig II.12: Ansys CFD-POST interface

II.12 Solidworks:

Even though the geometry of the project can be created using the properties of ansys system, we preferred in our project using the solidworks program (version 13.0) and then transfer the geometry to the ansys ICEM to generate the meshing.

Solidworks is computer software designed to create fast and accurate designs, including 3D models and 2D drawings of complex parts and assemblies.

A scheme of the simulation process is shown in figure II.13

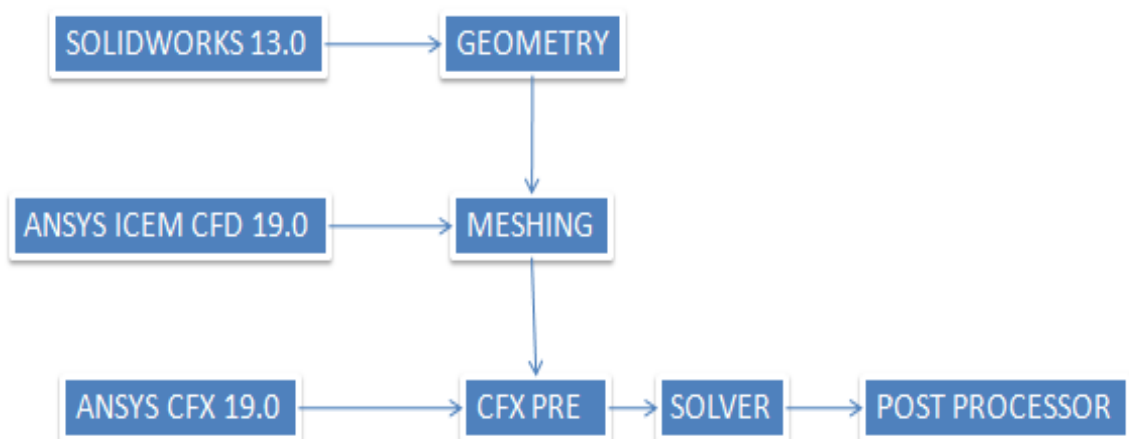


Fig II.13: Process scheme of the simulation

II.13 Finite volumes method:

The Ansys-CFX software utilizes the finite volumes method (FVM) to calculate the variation of velocity, temperature and pressure throughout the domain studied.

The Ansys code uses a technique that consists of integrating the differential equations on each control volume and then converting them into algebraic equations.

The finite volume method consists in dividing the computation domain into several volumes where each volume surrounds a node. By using different approximation schemes one can integrate the terms of the differential equations modeled on each control volume or the values and quantities are stored at the nodes of the control volume.

These produced algebraic equations express the conservation of quantities for the control volume and for the entire computational domain.

II.14 conclusion:

In this chapter the working principle of the gas turbine is presented. The different methods of increasing the performance of the turbine and enhancing the blades cooling efficiency by the use of film cooling technique are shown. . Finally the software used in the numerical simulation of the blade cooling is described.

Chapter III:
Study of a case

III.1 Introduction:

The great development in the field of computers contributed impressively to the development of simulation software, which allowed accurate studies to be carried out in a short time and at low costs. In this chapter, we present the steps of simulating the cooling of a turbine blade with cooling film method, using two software ANSYS and SOLIDWORKS.

III.2 Gas turbine blade modelling:

The blade geometries are generated using solid-works software which has an accurate and precise topology. The blade is constructed from an airfoil (Fig III.1).

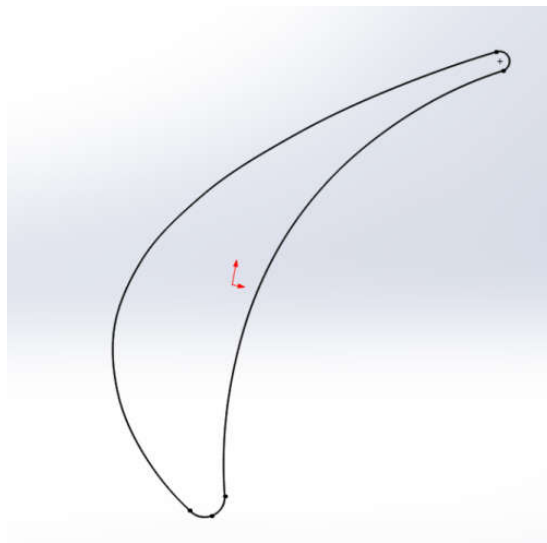


Fig III.1: blade airfoil-Solidworks

The airfoil design details are shown in the table III.1.

Table III.1: Airfoil design parameters:

Parameters	Value
Inlet angle α_1	41.42°
Outlet angle α_2	22.17°
Chord line length	32.6 mm
Camber line length	38.18 mm

In our simulation we made three distinct cases:

- First case: case (1) (Fig III.2)

The geometry has a height of 50mm.

This geometry represents a simple blade which is not cooled.

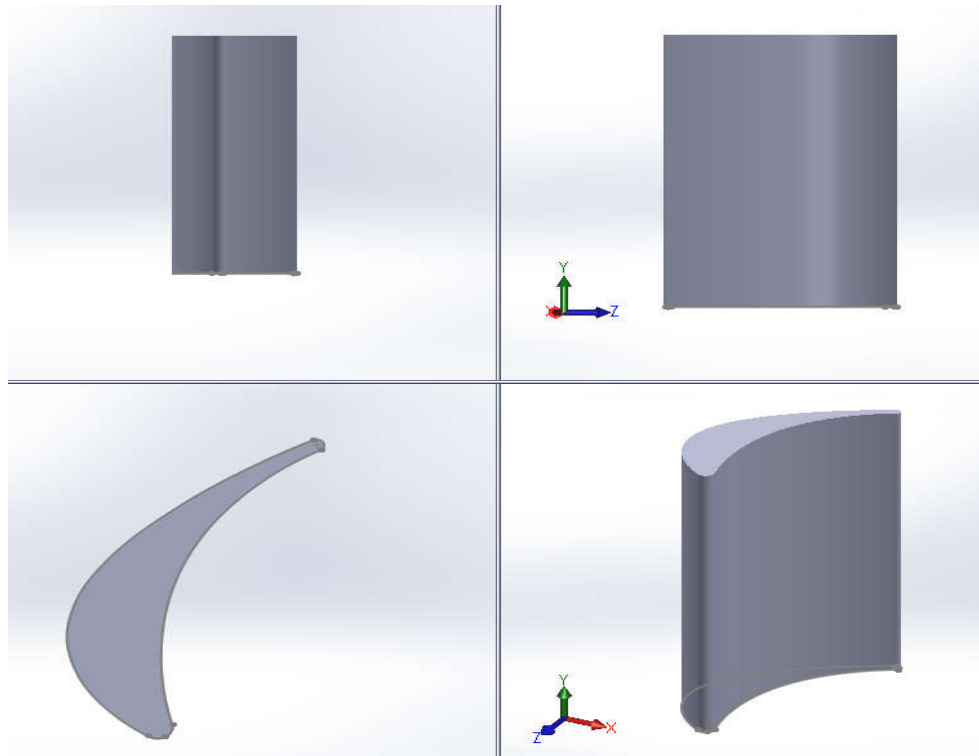


Fig III.2: Case(1) geometry design

Remark:The height is divided by 10 in the case (2) and (3) in order to simplify the simulation process and reduce the mesh elements number.

- Second case: case (2) (Fig III.3)

In this case three slots are added inside the blade in a longitudinal direction, which represents the cooling channels.

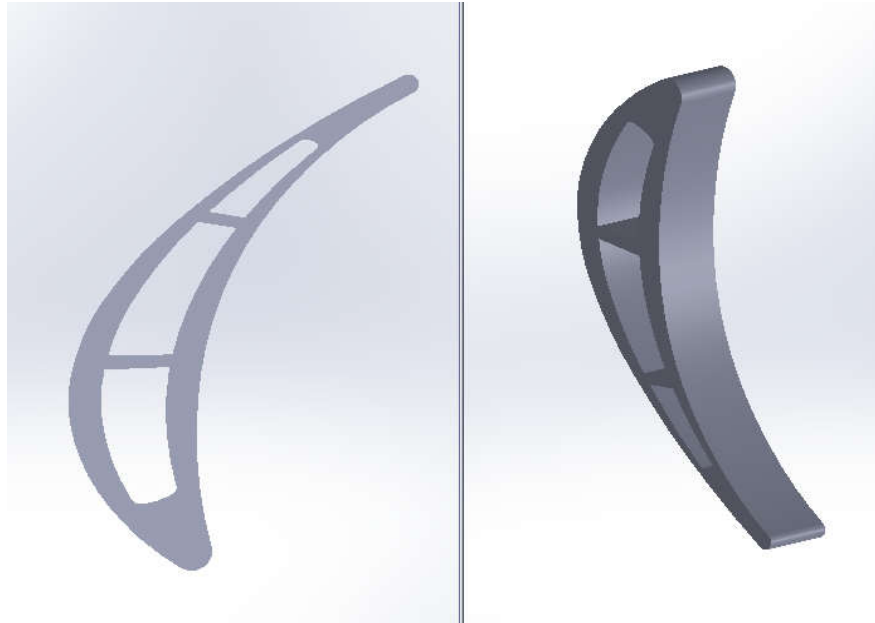


Fig III.3: Case(2)geometry design

➤ Third case: case (3) (Fig III.4)

As for the third case, cylindrical holes that would distribute the cooling air into the outside surface of the blade are added, where it will mix with the main stream flow (Fig III.4).

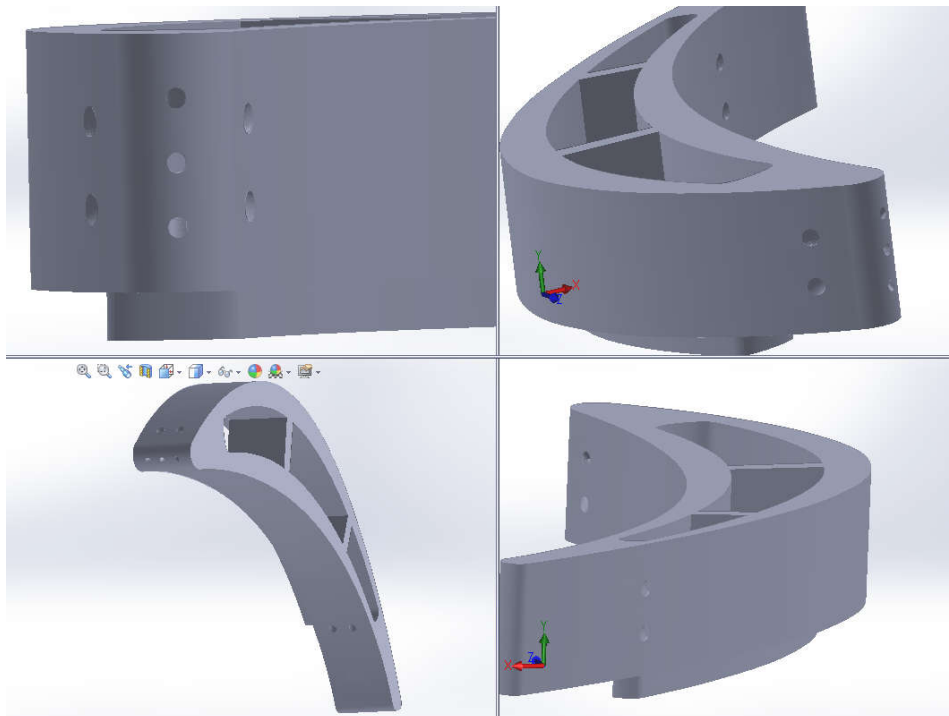


Fig III.4: Case (3)geometry design

The different characteristics of the holes added in the case (3) are shown in the table III.2

Table III.2: film cooling holes configuration

Holes region	Diameter	Injection angle
Tip	0.4mm	40°
Others	0.64mm	32°

The geometry of the hot air domain is designed in a way that simulates the field surrounding the turbine blade in order to obtain accurate results as shown in Figure III.5.



Fig III.5: Hot air domain geometry design.

The blade body is made of Stainless steel; its mechanical properties are shown in table III.3.

Table III.3: mechanical properties of Stainless steel

properties	Units	Stainless steel
E	Gpa	200
P	Kg/m ³	7750
K	W/m·k	15
M	---	0.29
Cp	J/kg·k	500
Melting point	°C	1530°
Yield stress	Mpa	215

III.3 Mesh generation:

After finishing the design of the cases, we export them to the ANSYS ICEM CFD Software for mesh generation process.

Cases (1) and (2) has been meshed using hexahedral structure meshing type, as shown in Figures III.9and III.11.

- The case (1) contains two domains; the solid body and the hot fluid, so we create two blocks then split those according to the geometry, then we associate vertexes to points(fig III.6), edges to curves(fig III.7) and faces to surfaces, and link edges to get accurate mesh. After that we set meshing parameters (scale factor, edge parameters) BiGeometric law is used, and finally converting to Unstruct mesh.

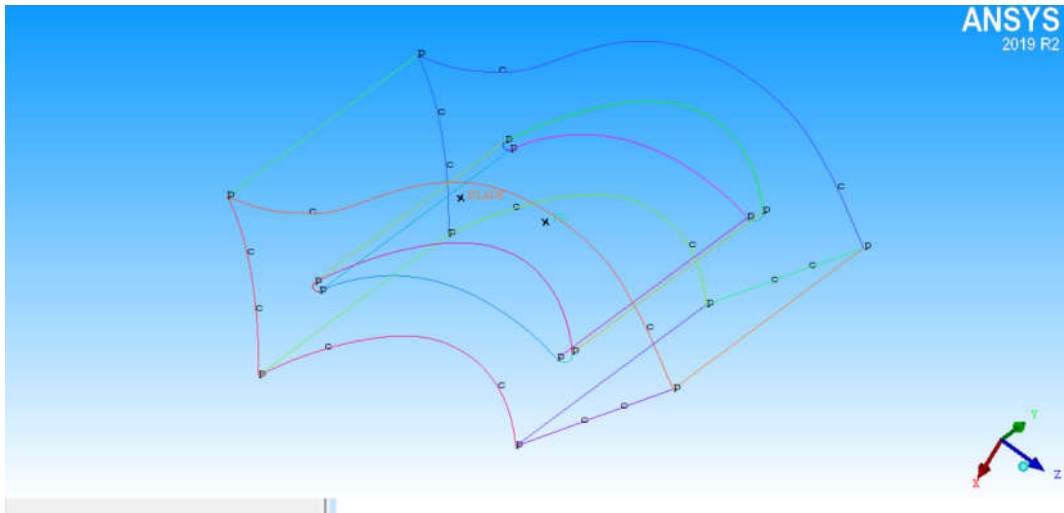


Fig III.6: Vertexes to points association

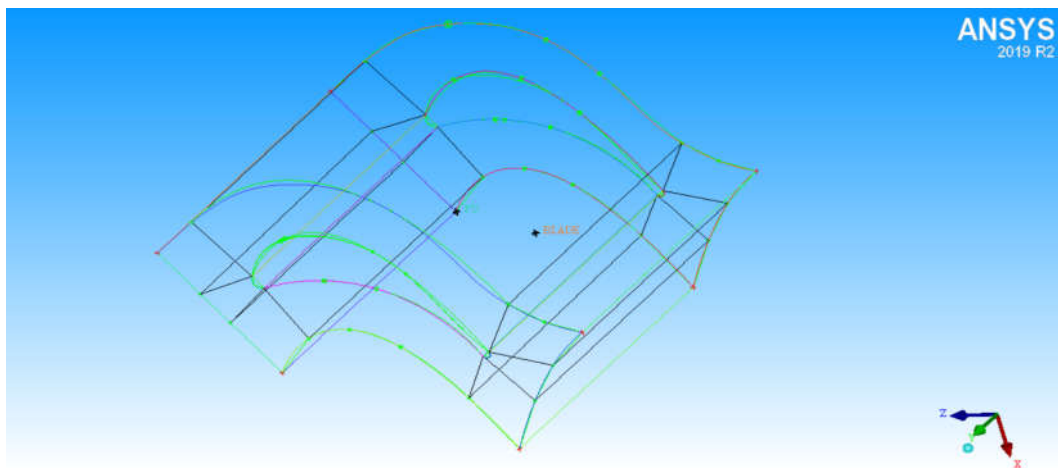


Fig III.7: Edges to curves association

Blocking of case (1) is shown in figure III.8.

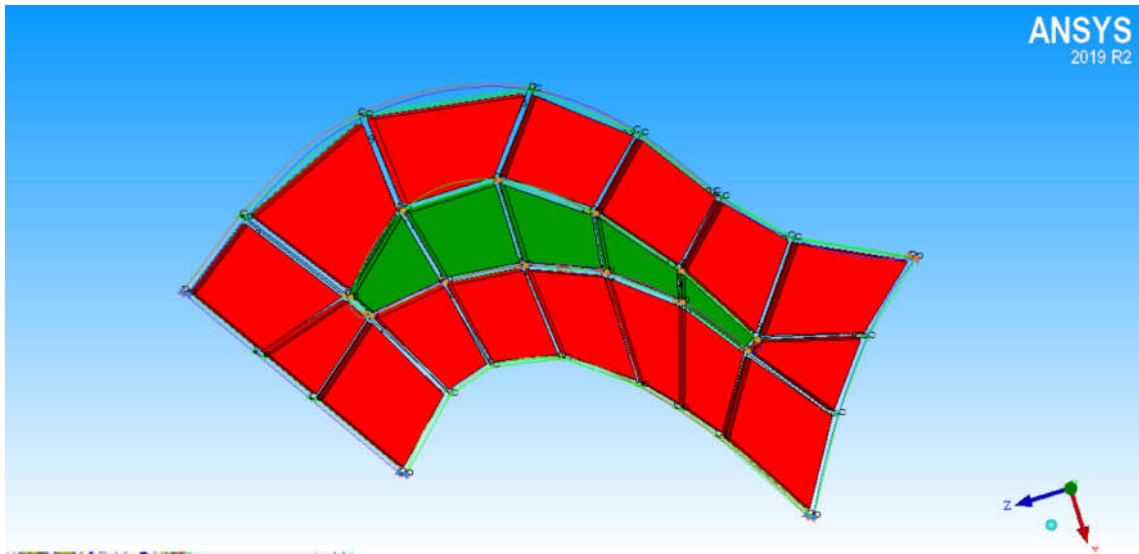


Fig III.8: Blocking of case (1)

Meshed domains for case (1) are shown in figure III.9.

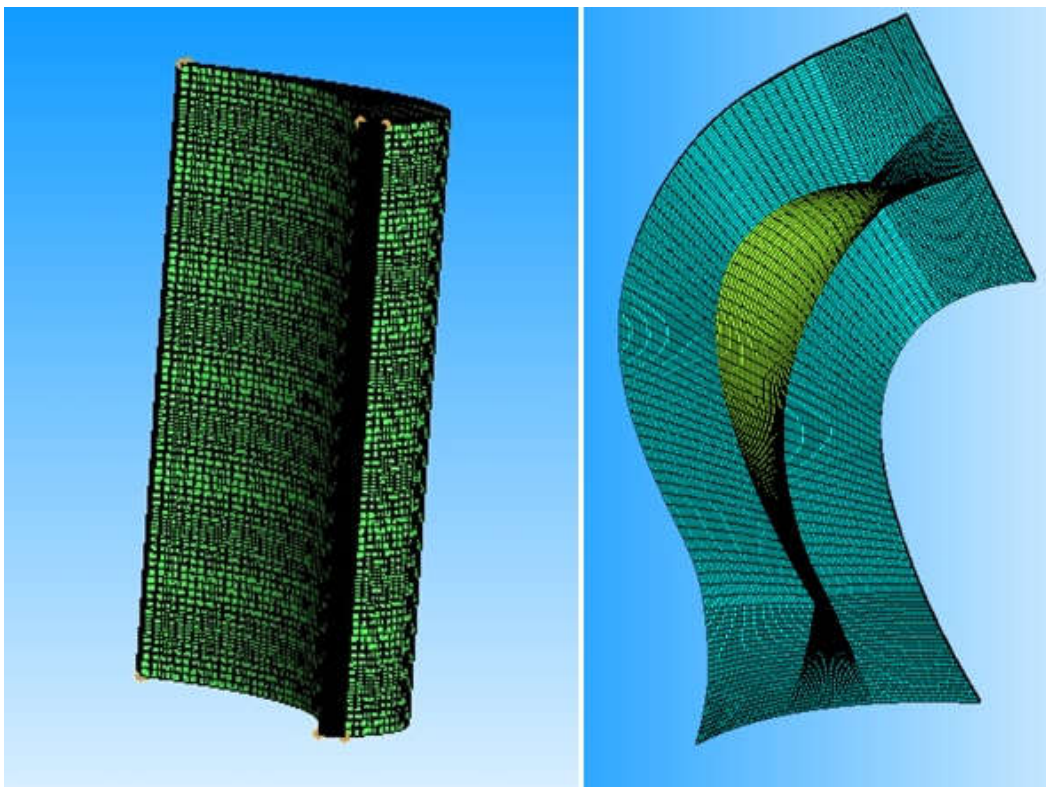


Fig III.9: Meshed domains for case(1)

The number of elements, nodes, and the quality of the mesh are shown in (table III.4)

Table III.4: Case (1) Mesh Details

<i>Total elements</i>	<i>Total Nodes</i>	<i>Mesh Quality</i>
666020	634700	

- Case (2), the same steps as case (1) has been applied; the only difference lies in that a coolant fluid domain is add to the two existing domains, the solid and hot fluid domain,(fig III.10)

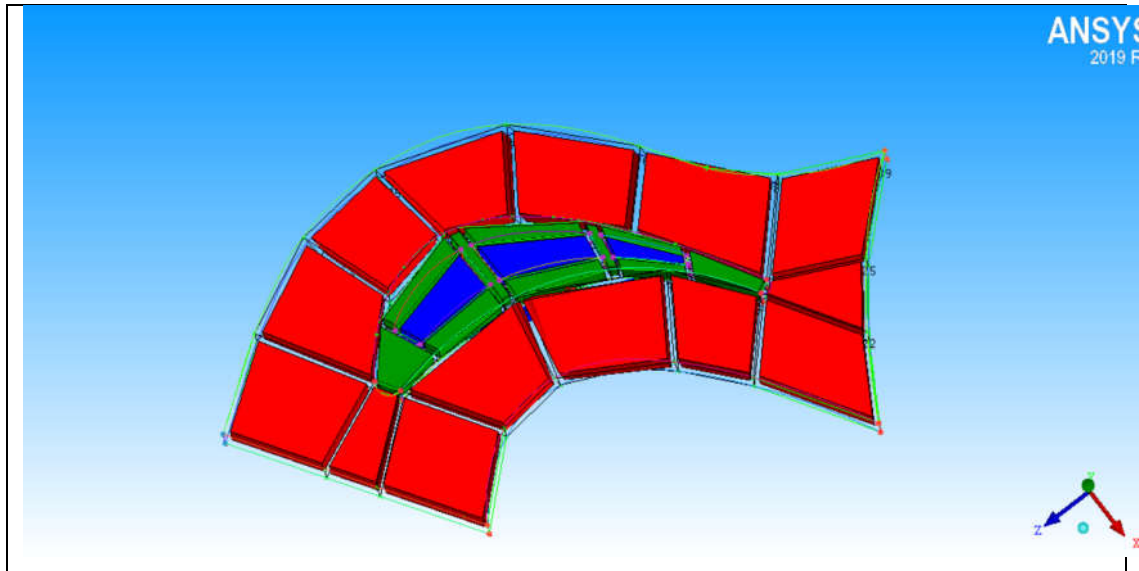


Fig III.10: Blocking of case (2)

Meshed domains for case (2) are shown in figure III.11

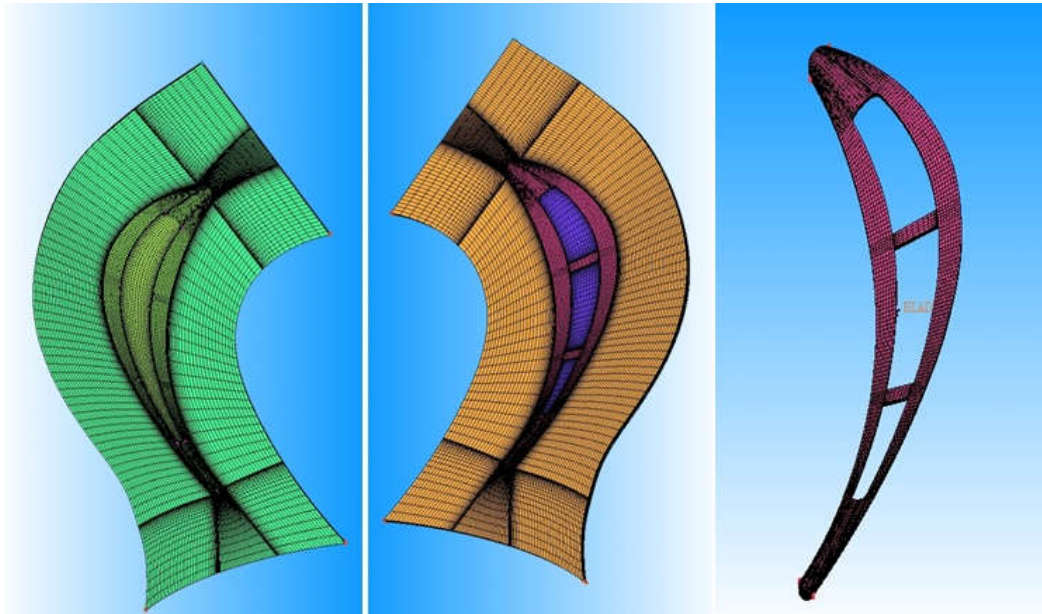


Fig III.11: Meshed domains for case(2)

The number of elements, nodes, and the quality of the mesh are shown in (table III.5)

Table III.5: Case (2) Mesh Details

<i>Total elements</i>	<i>Total Nodes</i>	<i>Mesh Quality</i>
175647	151430	

- Case (3), in the third case we have a complex geometry design, the holes and cylindrical tubes in the blade body make the process of blocks splitting difficult, so we found the tetrahedral type meshing better to save time. But the tetra meshing has its disadvantage, it is not very precise in the curvature or holes areas, so we made it hybrid, we meshed the holes tubes with hexahedral (Fig III.12), and the rest of the model with tetra in order to combine time, gain and accuracy (Fig III.13).

So firstly we set global mesh size which the scale factor parameter is 1, then part mesh setup, prism meshing parameters, surface mesh setup (the tail and the tip), also we set curves mesh parameters to capture the features of the curves, and finally computing

the mesh by selecting volume mesh compute, Tetra/mixed type , robust(octree) method. Then the tubes hexahedral mesh and tetrahedral mesh has been merged (volume, surface) using merge nodes features to make all mesh consistent.

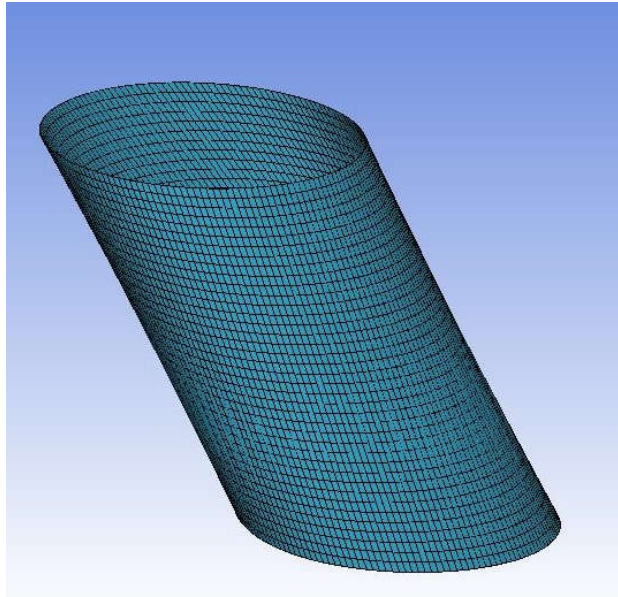


Fig III.12: Tube hexahedral mesh

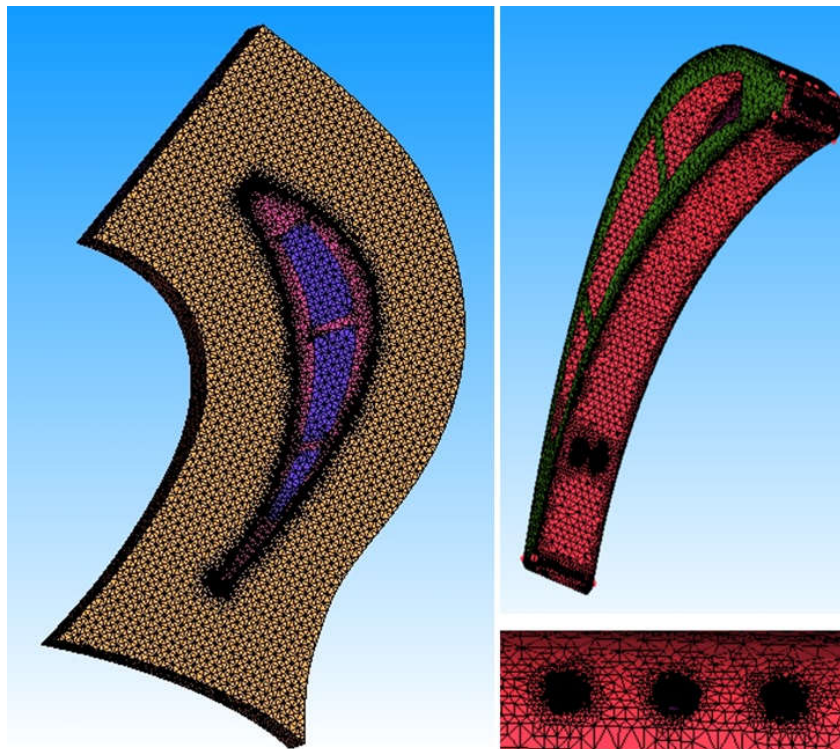


Fig III.13: Meshed domains for case(3)

The number of elements, nodes, and the quality of the mesh for case (3) are shown in (table III.6)

TableIII.6: Case(3) Mesh Details

<i>Total elements</i>	<i>Total Nodes</i>	<i>Mesh Quality</i>
1772197	376403	

Remark: in order to get more precise results an adjustment of the meshing(refinement) is required in some areas of the geometry such as the interfaces and holes.(fig III.14) and (fig III.15)

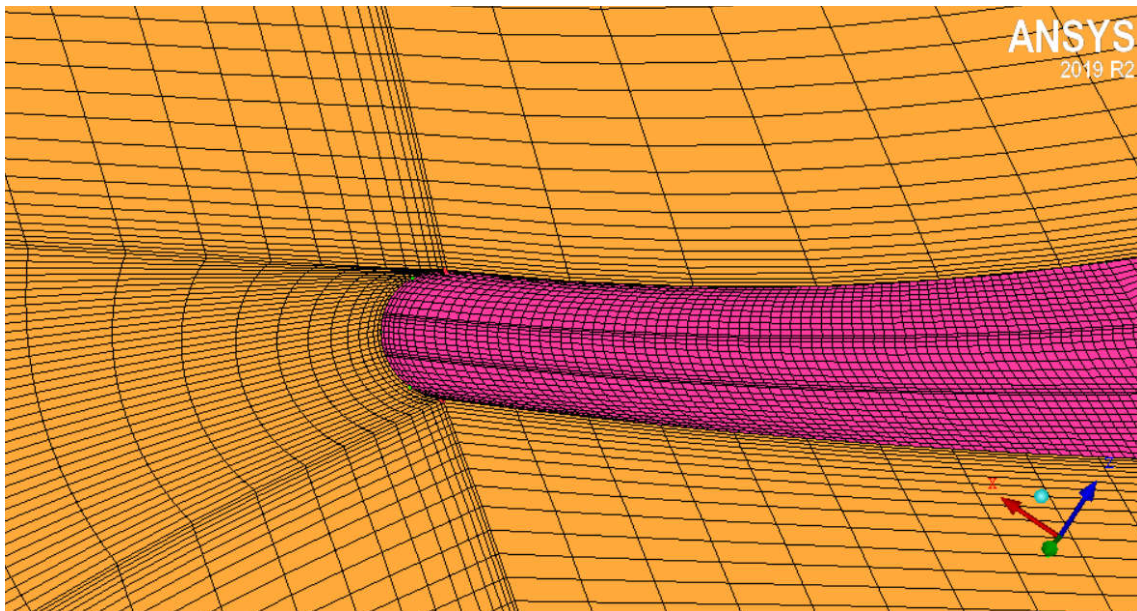


Fig III.14: Mesh refinement at leading edge (view1)

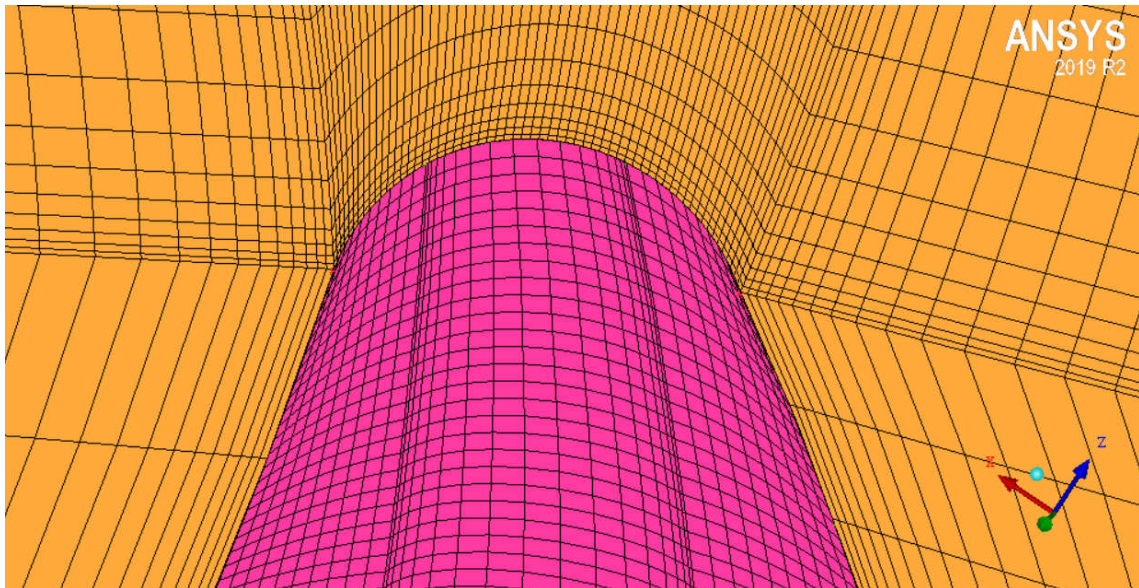


Fig III.15: Mesh refinement at leading edge (view2)

III.3.1 Mesh study:

To obtain more accurate results from the meshing and find the optimal mesh configuration, a mesh study has been made, where we tried five different meshes with different numbers of nodes and elements and checked the results of the pressure given by each mesh.

The five meshes details are shown in (table III.7).

Table III.7: Mesh study details:

	Elements	Nodes
Mesh 1	27562	25423
Mesh 2	54236	52856
Mesh3	93364	91254
Mesh4	175647	151430
Mesh 5	385721	359839

The results of the mesh study are shown in the graph in (figure III.16).

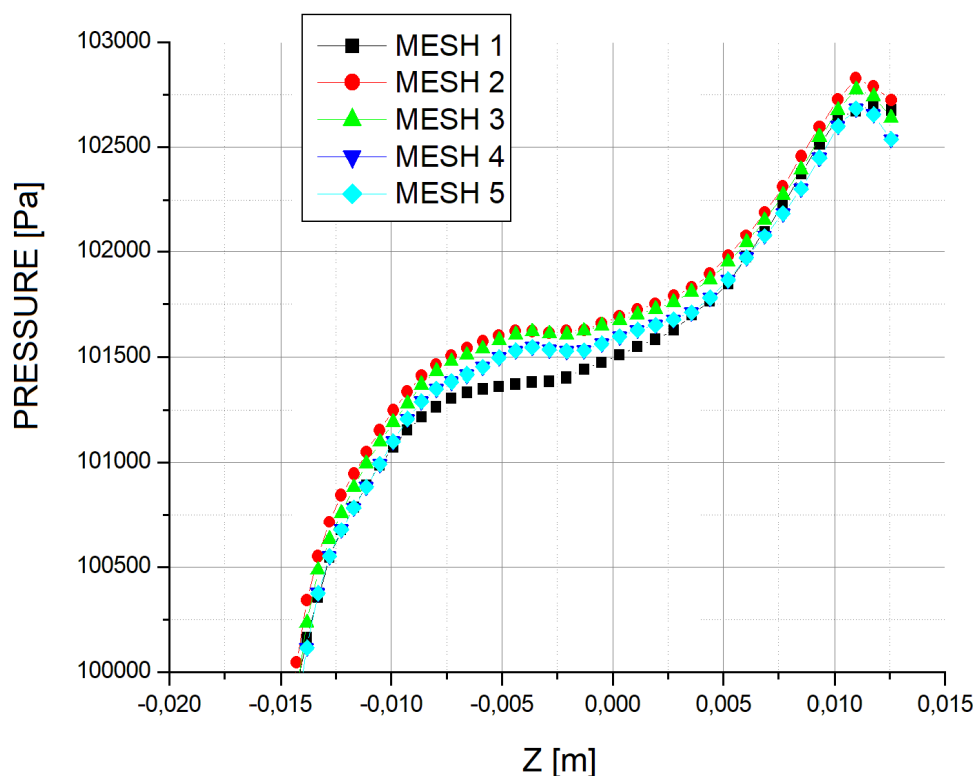


Fig III.16: The pressure graphs given by the different meshes.

From the results shown in (figure III.16), we found that mesh 4 and mesh 5 graphs are almost identical. Therefore we conclude that mesh 4 will offer accurate results with optimal number of elements and nodes.

III.4 Pre processing:

The mesh is exported from ICEM software in **.CFX5** extension to CFX.PRE interface in order to define the simulation data settings and physical parameters to describe the flow problem and specify the boundary conditions.

III.4.1 Domains inputs:

The fluid material in hot flow and coolant domains is Air ideal gas with a 1 [atm] as a reference pressure and the solid is stainless steel. The heat transfer option is a thermal energy.

III.4.2 Boundary condition:

The table III.8 presents all boundary conditions parameters that are applied:

Table III.8: Boundary conditions input

Parameters	Values
Hot air inlet velocity (m/sec)	100
Hot air inlet temperature (k)	1425
Coolant inlet velocity (m/s)	45.11
Coolant inlet temperature (k)	300
Turbulence	K-epsilon
Intensity	5%

III.4.3 Interfaces:

- Case 1: two interfaces, rotational periodicity, and fluid-solid interface which is the hot flow blade contacting surface.(figure III.17)
- Case 2: three interfaces, rotational periodicity, and two fluid-solid interfaces; the blade contains external interface with hot flow and internal interface with coolant.(figure III.18)
- Case 3: the some previous interfaces plus a fluid-fluid interface which represent the hot flow and coolant contact surface.(figure III.19)

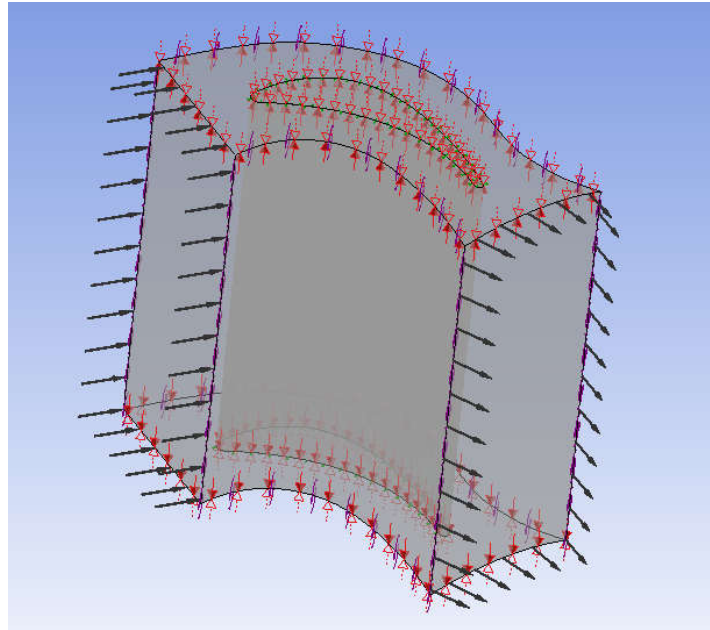


Fig III.17: Case(1) Pre-processing

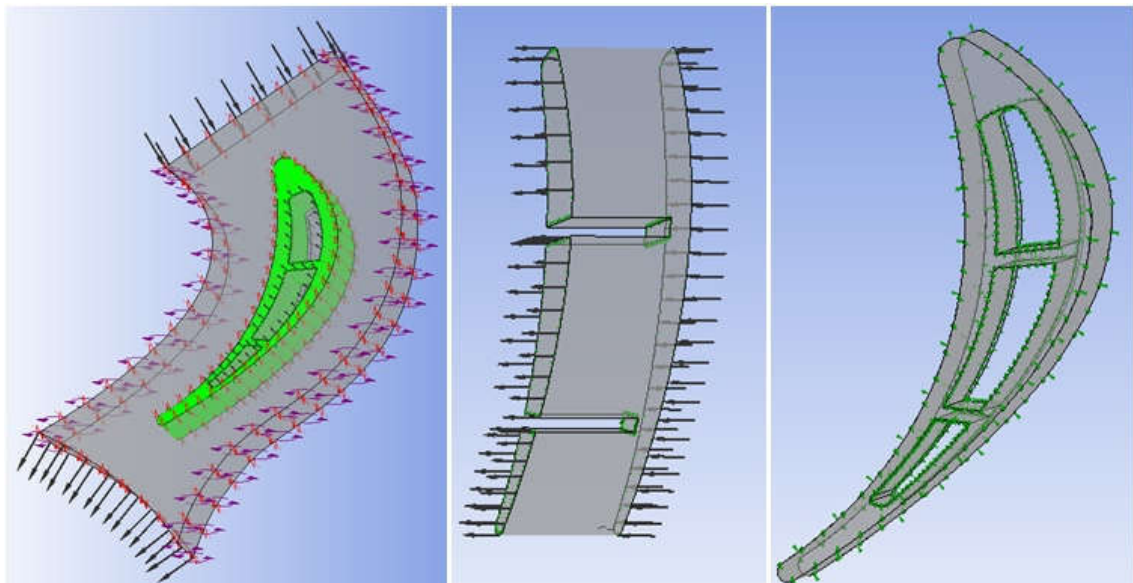


Fig III.18: Case(2) Pre-processing

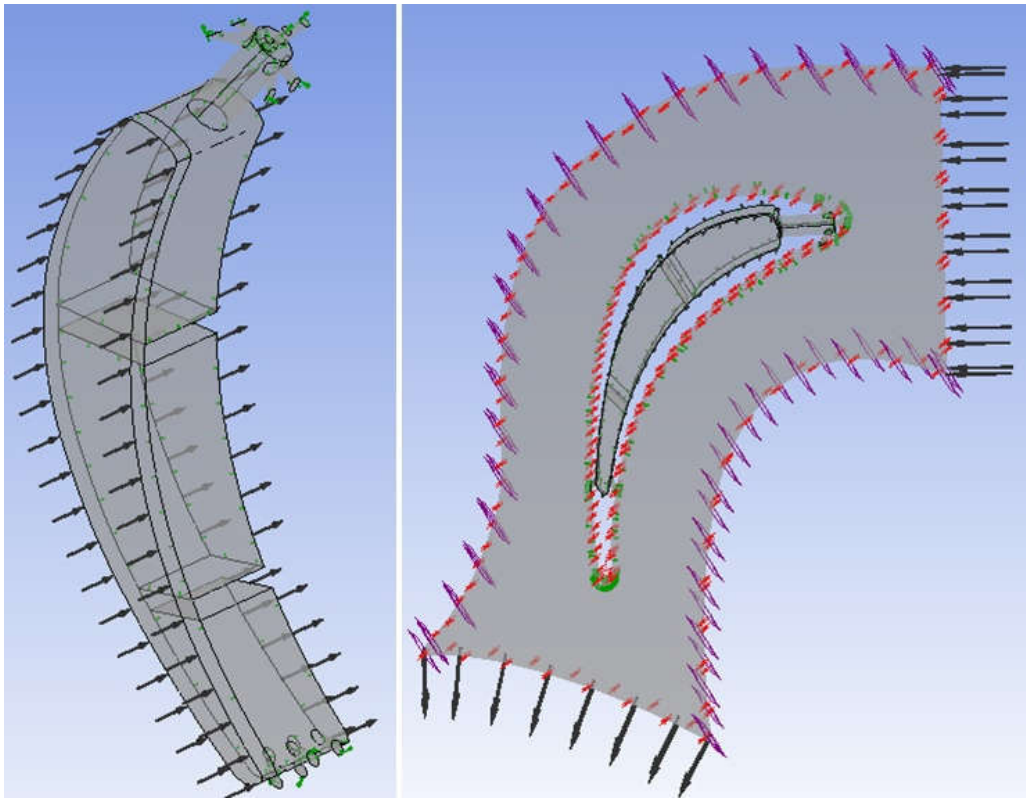


Fig III.19: Case(3) Pre-processing

III.4.4 Solver control:

In solver control, the residual target is 10^{-5} .

III.5 CFX-POST:

After completing the calculation process, the results are treated in CFX-CFD-POST.

III.6 Conclusion:

In this chapter, we have presented in an important and detailed manner all the necessary steps taken to simulate the process of cooling the turbine blade using cooling film techniques, where we presented three cases (1), (2) and (3) of complementary geometric designs. The steps are summarized as follows:

- Models geometric design using SOLIDWORKS software.
- Mesh generation using ICEM CFD software.
- Models data preparation in CFX PRE interface.
- Results treatment with CFX-CFD-POST.

Chapter IV:
Results and discussion

IV.1 Introduction:

This chapter relates to the analysis and discussion of the results of the process of cooling the turbine blades using coolant passing through internal channels. The boundary conditions applied in this simulation are similar to experimental results of gas turbine carried out by **Khaled Al-Farhany[25]**. The performance of the cooling system is evaluated using temperature distribution (contours, charts) and cooling effectiveness η . The study consists of blade geometry design improvement using convection and cooling film techniques. Three cases have been studied, case (1) the blade as it is without cooling, case (2) three internal slots for the cooling are installed and for case (3) additional cylindrical holes are insert from the internal slots to the blade surface, so the coolant air escapes from.

IV.2 Results analyses of temperature and heat flux distribution:**IV.2.1 Case 1:**

Figure IV.1 present contour of temperature for blade surface in case 1. It is found that the blade temperature is equal to 1425 K that represents the inlet mainstream temperature which is coming from combustion chamber. Blade and hot air are in thermal equilibrium; that means the total heat transfer rate by convection is null as shown in figure IV.2. So case 1 is basically a definition of the problem being studied.

The main goal is reducing the temperature at the blade surface by injecting coolant fluid passing through the blade body.

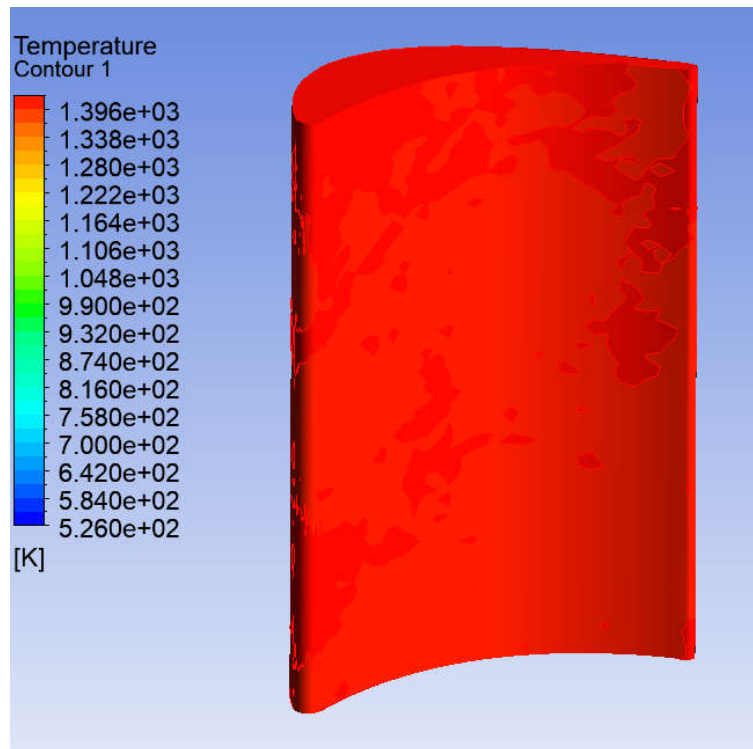


Fig IV.1: Contour of temperature for blade surface case (1)

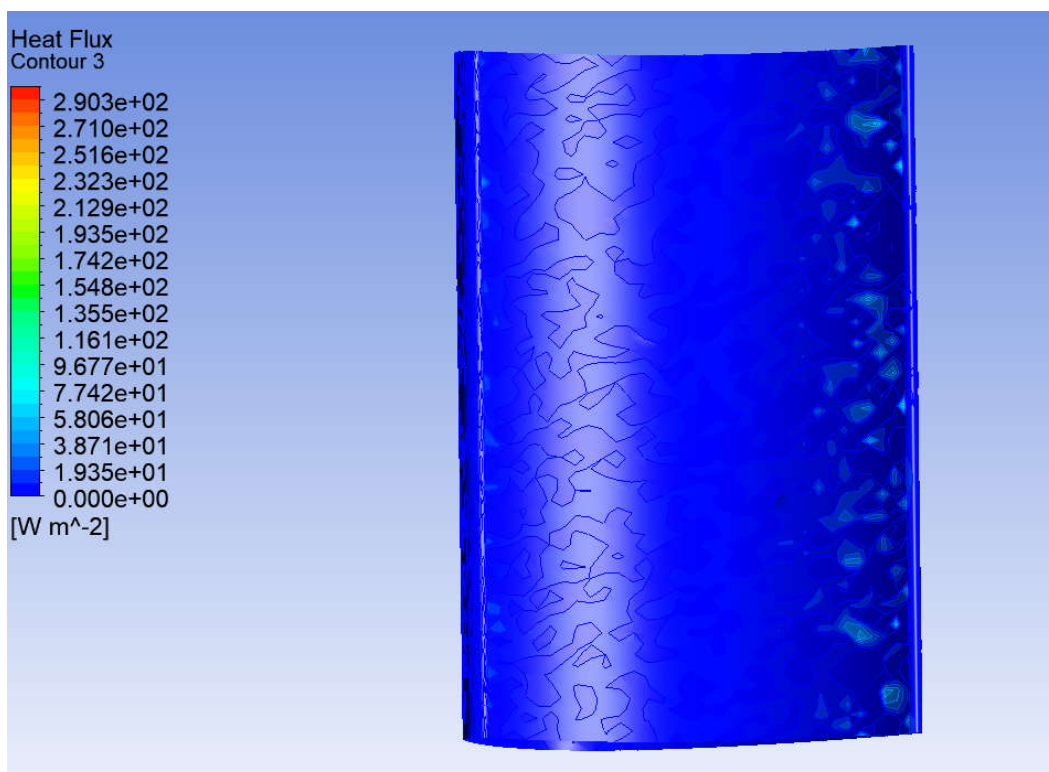


Fig IV.2: Contour of heat flux for blade surface case (1)

IV.2.2 Case 2:

Figure IV.3 present contour of temperature for blade surface. It is observed that there is a decrease in blade temperature, it reached a maximum value of 1098 K at leading and trailing edges regions, and minimum of 976 K at med chore section.

The leading and trailing edges regions are the most sensitive to high temperature affect, because the leading edge located at stagnation region and it faces the mainstream inlet coming from the combustion chamber with high temperature and the trailing edge is thin and confronting the hot flow emission.

The figure IV.4 show contour of heat flux for blade surface. It is found that the total heat transfer rate by convection increased to an average value of $108258 [W/m^2]$, because the coolant passes in internal slots through the blade cavity and leads to decreasing the temperature at blade surface.

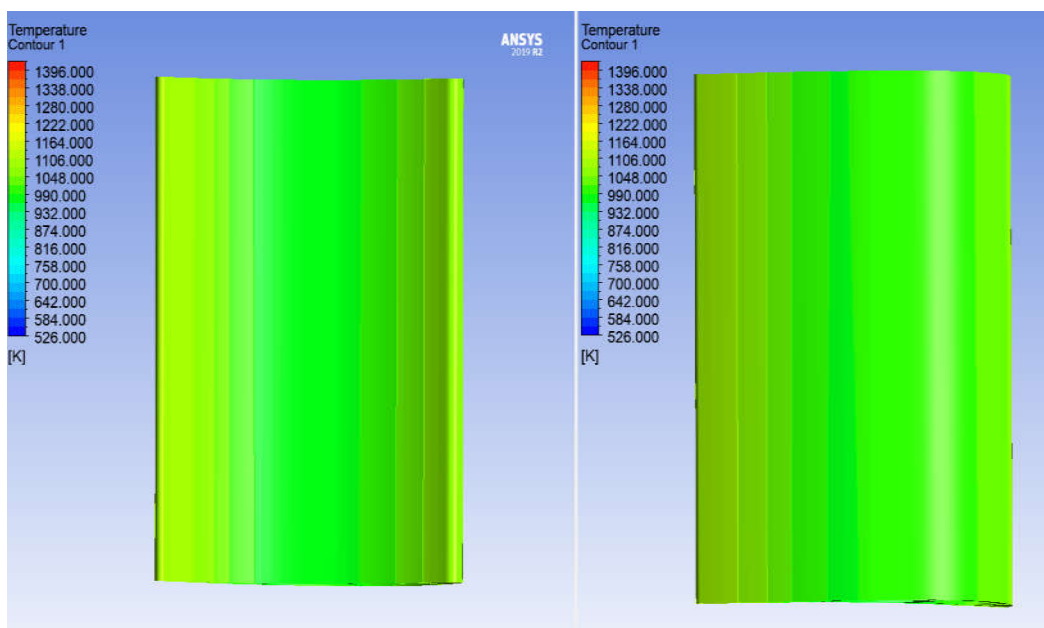


Fig IV.3: Contour of temperature for blade surface case 2

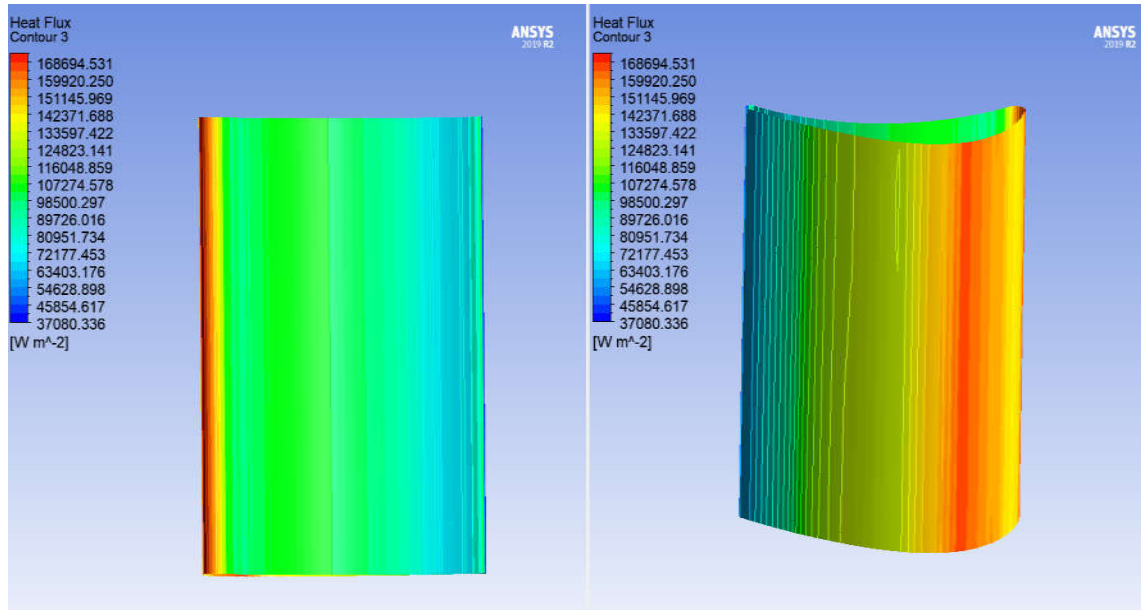


Fig IV.4:Contour of heat flux for blade surface case (2)

IV.2.3 Case 3:

The figure IV.5 presents contour of temperature for blade surface. It is observed that there is a significant decrease in blade surface temperature where it reached a maximum value of 635 K at leading and trailing edges regions, and minimum of 526 k at med chore section. However, the total heat transfer rate by convection increased to an average value of 196954 [W/m^2], because the coolant passes in internal slots through the blade body, and the protective layer which is created by exiting coolant from the holes in direction of mainstream. The layer effect is reducing the heat transfer from the hot gas to the blade surface, which leads to decrease the temperature at blade surface, figure IV.6.

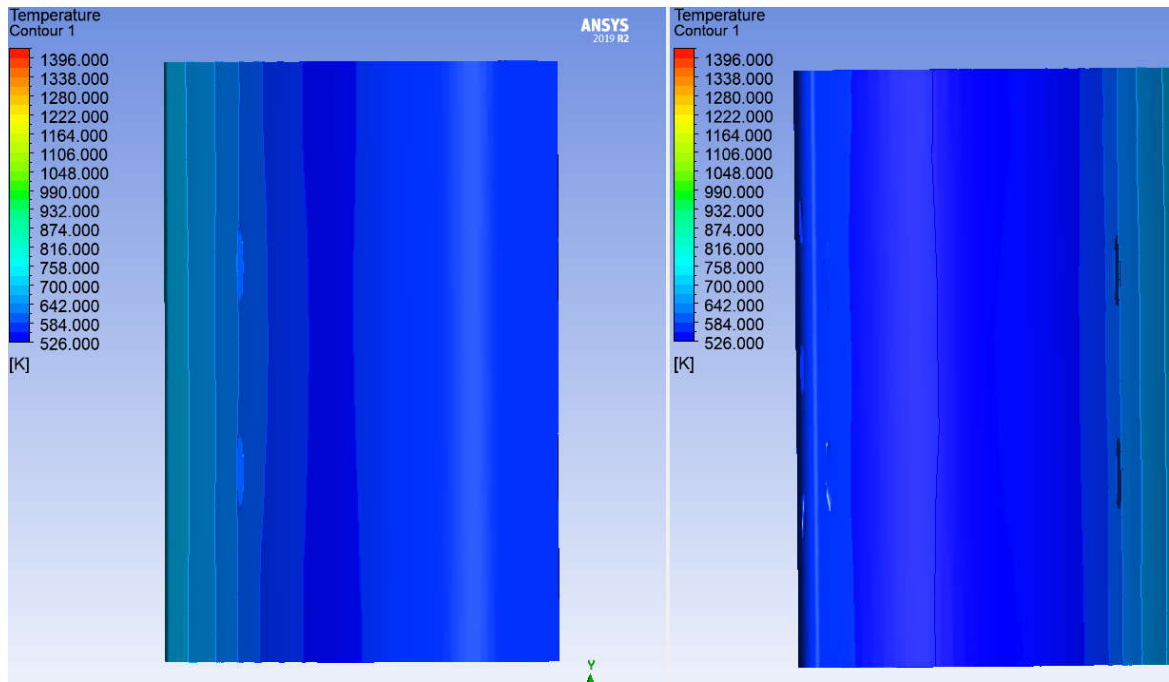


Fig IV.5: Contour of temperature for blade surface case (3)

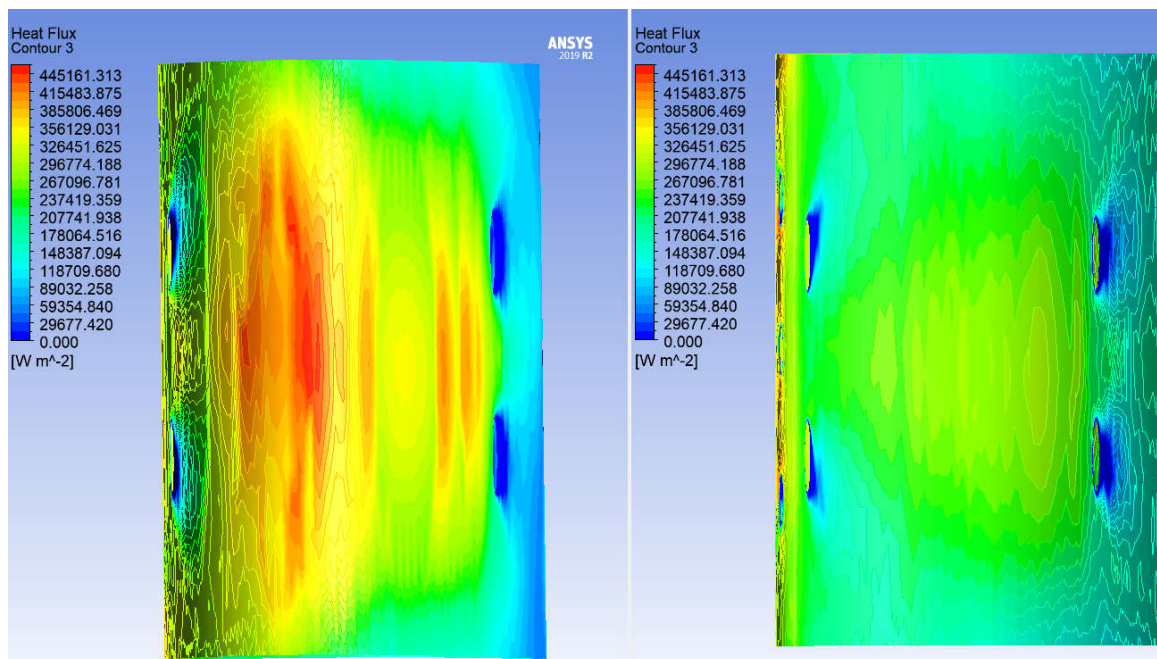


Fig IV.6: Contour of heat flux for blade surface case (3)

The figure IV.7 presents the temperature distribution at intrados polyline for the second and the third cases compared to the reference case (case 1). It is shown that the temperature decreased in case 2 from 1425 K to 1098 K at leading edge region and 950 K at med chore section and 1091 K at trailing edge region. In case 3, the temperature decreased from 1425 K to 680 K at leading edge region and 530 K at med chore section and 575 K at trailing edge region.

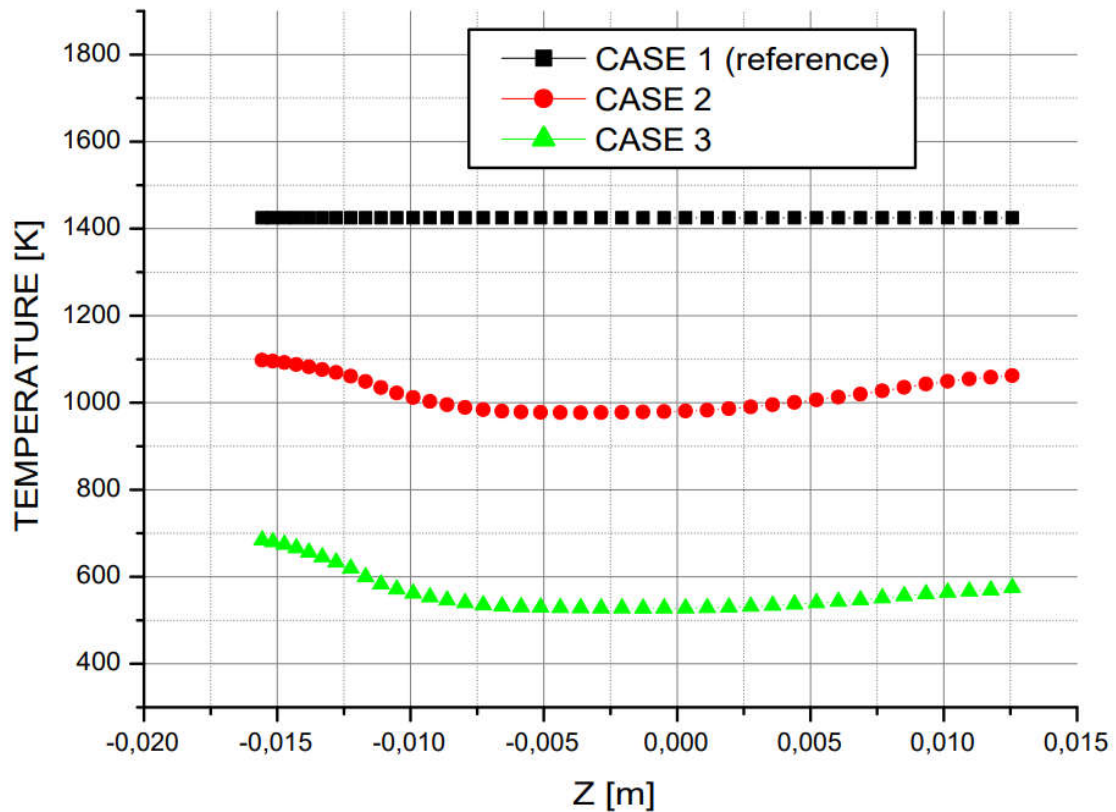


Fig IV.7: Temperature distribution at intrados polyline for the three cases

The figure IV.8 presents the temperature distribution at intrados polyline for the second and the third cases compared to the reference case (case 1). It is shown that the temperature decreased in case 2 from 1425 K to 1098 K at leading edge region and 975 K at med chore section and 1050 K at trailing edge region. In case 3, the temperature decreased from 1425 K to 680 K at leading edge region and 530 K at med chore section and 575 K at trailing edge region.

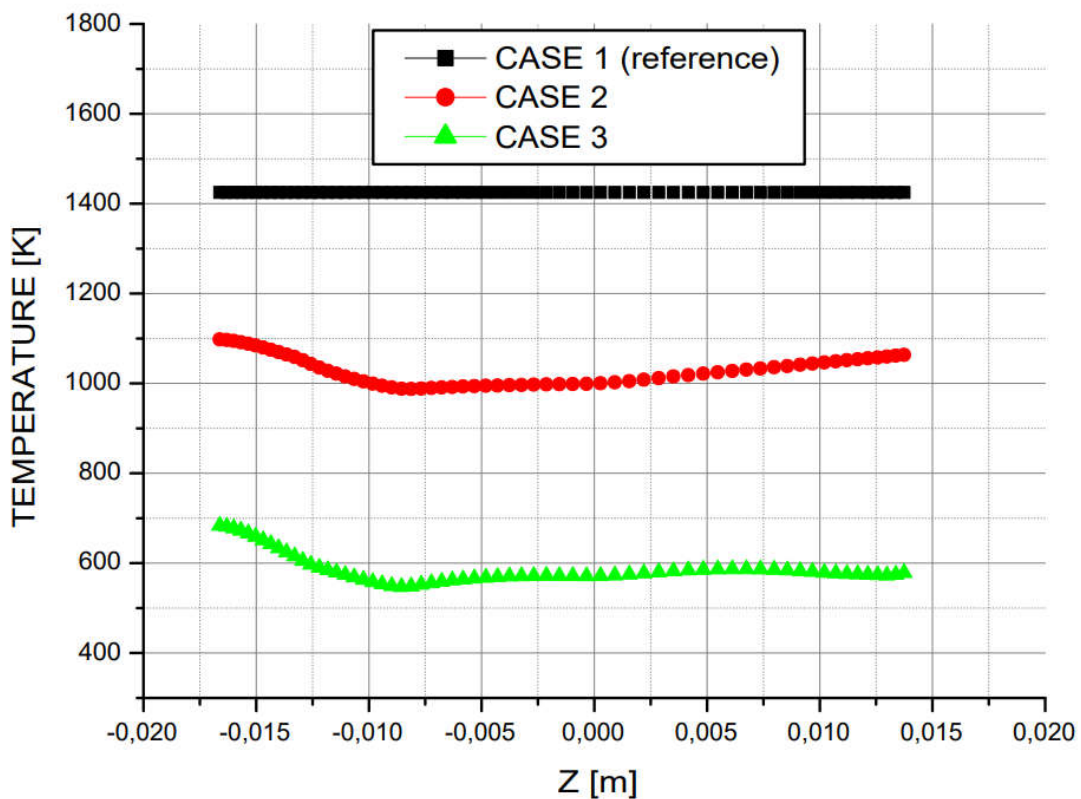


Fig IV.8: Temperature distribution at extrados polyline for the three cases

The figure IV.9 shows the coolant flow layer on the blade surface with the calculated blowing ratio of $M=0.54$. The coolant passes by internal slots and exit from the holes covering the blade surface by a layer in order to protect it against the high temperature. This leads to a reduction of blade surface temperature and an increase in the total heat transfer rate and thus obtaining high cooling efficiency.

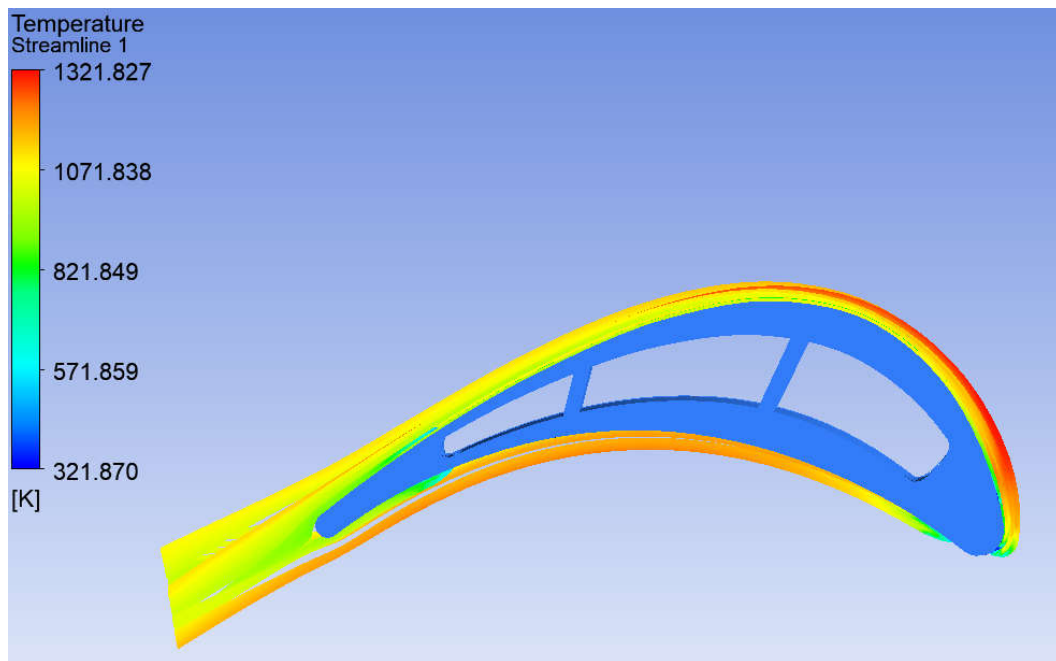


Fig IV.9: Coolant temperature streamlines

IV.3 Results analyses of effectiveness:

The figure (Fig IV.20) presents the cooling effectiveness η contours and charts for cases (2) and (3). It's observed that in case (2) the max value of efficiency reached 39.8% and 29% as the minimum. In case (3) we see significant improvement, in which the max efficiency value increases to 79.8% and 65.7% as the minimum value.

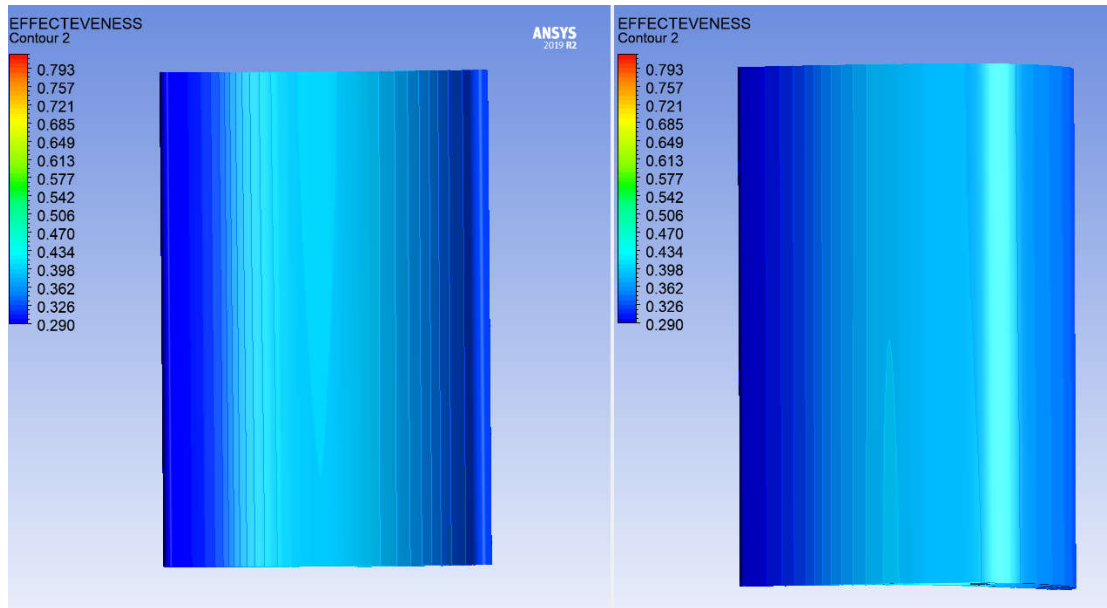


Fig IV.10: Cooling effectiveness η distribution for case (2)

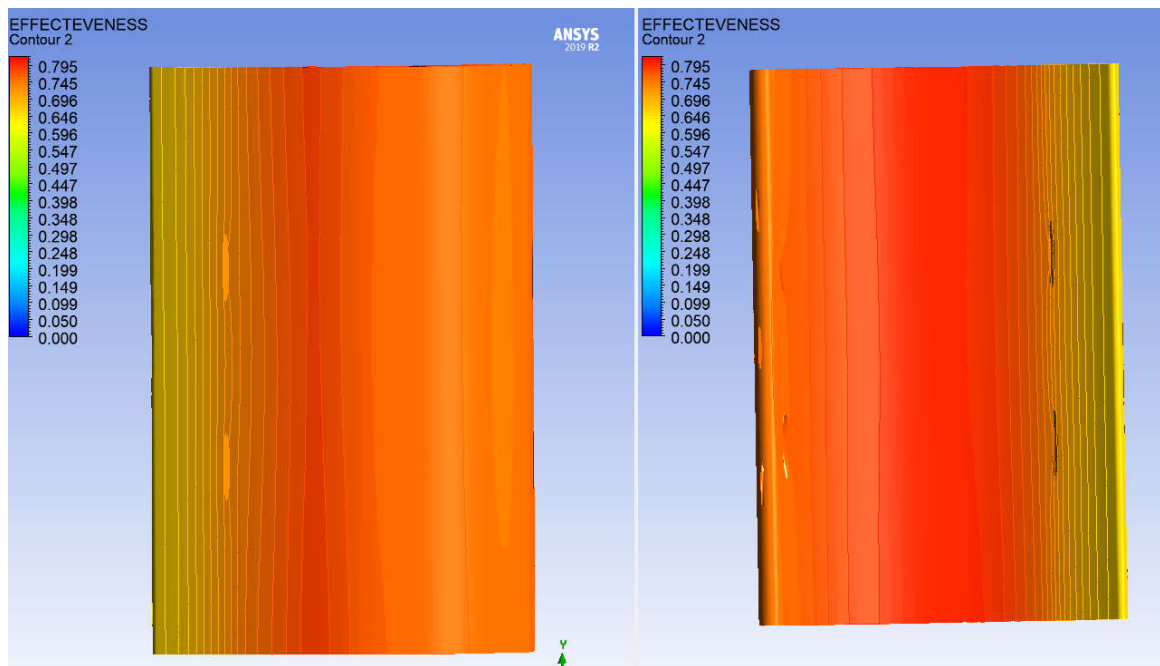


Fig IV.11: Cooling effectiveness η distribution for case (3)

The figure IV.12 presents the cooling effectiveness η variation at intrados polyline for case (3) compared with the case (2). It is shown that the effectiveness increase from 29% to 65% at trailing edge region and from 39.8% to 79 % at med chore section then from 34% to 75 % at leading edge region.

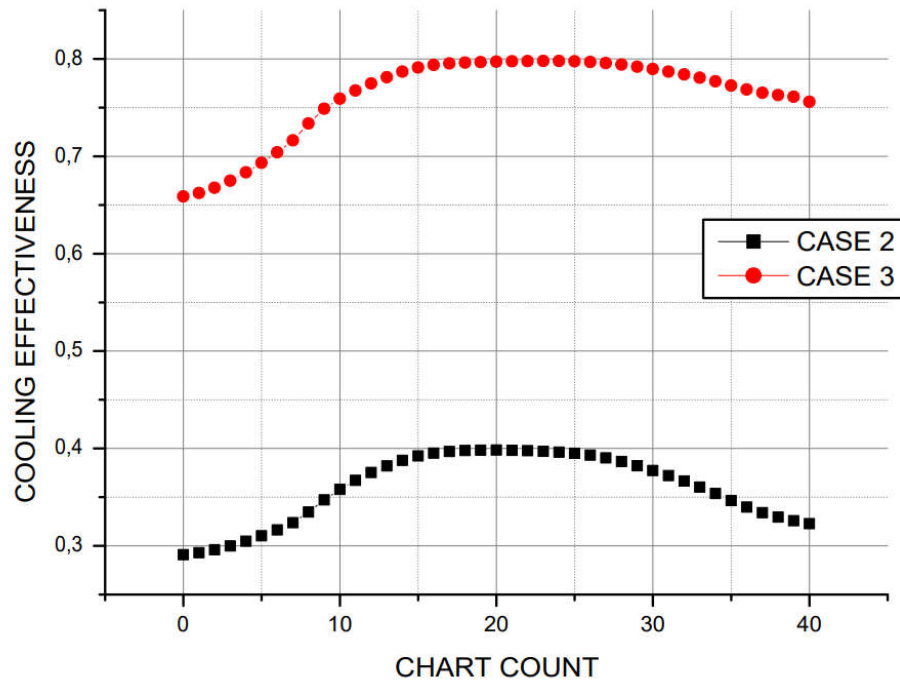


Fig IV.12: Cooling effectiveness η variation at intrados polyline for case 2 and 3

The figure IV.13 presents the cooling effectiveness η variation at extrados polyline for case 3 compared with case 2. It is shown that the effectiveness increase from 32% to 75% at leading edge region and from .38% to 77 % at med chore section then from 28 % to 65 % at trailing edge region.

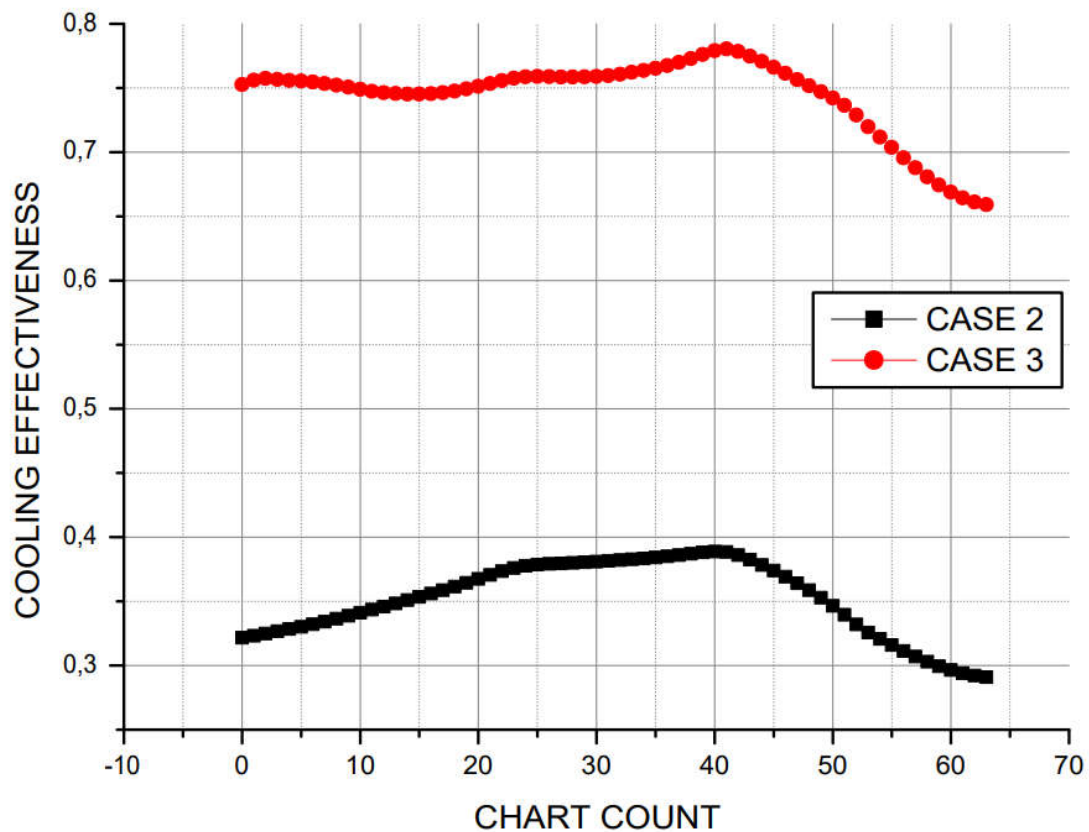


Fig IV.13: Cooling effectiveness η variation at extrados polyline for case 2 and 3

IV.4 Conclusion:

In this chapter we discuss the results of turbine blade cooling simulation. It is found that the case (3) is optimum, because the blade temperature reduced by about 55.43% and cooling effectiveness η reached 79%, that means the heat transfer from coolant flow to blade increased and heat transfer from hot flow to blade decreased.

General conclusion

General conclusion:

In this study, a detailed discussion and analysis of the turbine blade cooling process simulation using cooling film techniques has been accomplished. The main objective of this study is to provide a comprehensive understanding of this process and its impact on improving turbine performance.

In the first chapter of literature review, the work carried out in film cooling technique by few researchers is presented, the influence of some important parameters such as the shape, the angle of the cooling holes, the number of cooling jet rows, the blowing ratio are shown.

In the second chapter the working principle of the gas turbine is presented. The different methods of increasing the performance of the turbine and enhancing the blades cooling efficiency by the use of film cooling technique are shown. . Finally the software used in the numerical simulation of the blade cooling is described.

In the third chapter, we have presented in an important and detailed manner all the necessary steps taken to simulate the process of cooling the turbine blade using cooling film techniques, where we presented three cases of complementary geometric designs.

In the last chapter, numerical simulation results are discussed. The impact of the film cooling technique on the turbine blade temperature is shown. The efficiency of film cooling reaches 79% and the temperature of the blade is up to of 600 K.

References:

[1] Prashant B.Kuyate¹, Prof.N.C.Ghughe², Prof.D.D.Palande³, Prof.V.S.Daund⁴ “A Review on Film Cooling; Methods, Procedures, Analysis”

[2] S. Friedrichs, H. P. Hodson and W. N. Dawes, “Distribution of Film Cooling Effectiveness on a Turbine Endwall Measured Using the Ammonia and Diazo Technique” International Gas Turbine and Aeroengine Congress & Exposition, Houston Texas;(1995)

[3] Daniel G Hyams and James H Leylek, “A Detailed Analysis of Film Cooling Physics Part III: Streamwise Injection with Shaped Holes” International Gas Turbine and Aeroengine Congress & Exhibition, Florida; (June 1997)

[4] Srinath V Ekkad, Je-Chin Han and Hui Du, “Detailed Film Cooling Measurements on a Cylindrical Leading Edge Model: Effect of Freestream Turbulence and Coolant Density” International Gas Turbine and Aeroengine Congress & Exhibition, Florida; (June 1997)

[5] K. T. McGovern, J. H. Leylek, “A Detailed Analysis of Film Cooling Physics: Part II – Compound – Angle Injection with Cylindrical Holes” Journal of Turbo machinery; vol.122, (January 2000)

[6] J. E. Sargison, S. M. Guo, M. L. G. Oldfield, G. D. Lock, A. J. Rawlinson, “A Converging Slot-Hole Film-Cooling Geometry – Part 1: Low Speed FlatPlate Heat Transfer and Loss” Journal of Turbomachinery; vol.124, (July 2002)

[7] Dibbon K. Walters and James H. Leylek, “A Detailed Analysis of Film Cooling Physics Part I: Stream-wise Injection with Cylindrical Holes” International Gas Turbine & Aeroengine Congress & Exhibition; Florida, (1997)

[8] Younggi Moon, Soon Sang Park, Jung Shin Park, Jae Su Kwak, “Effect of Angle between the Primary and Auxilary Holes of an Anti-Vortex Film Cooling hole” Asia-Pacific International Symposium on Aerospace Technology (2014)

[9] Guangchao Li, Chaolin Wu, Wei Zhang, Zhihai Kou, DaweiPeng, “Effect of Cross-flow direction of Coolant on Film Cooling Effectiveness with OneInlet and Double Outlet Hole Injection” propulsion and Power Research; (2012)

[10] Xueying Li, Jing Ren, Hongde Jiang, "Film Cooling Effectiveness Distribution of Cylindrical Hole Injections at Different Locations on a Vane Endwall" *International Journal of Heat and Mass Transfer*, (2015);

[11] Xueying Li, Jing Ren, Hongde Jiang, "Multi-row Film Cooling Characteristics on a Vane End-wall"

[12] Xing Yang, Zhao Liu, Zhansheng Liu, ZhenpingFeng, "Numerical Analysis on Effects of Coolant Swirling Motion on Film Cooling Performance" *International Journal of Heat and Mass Transfer*, (2015).

[13] Low-pressure axial compressor scheme of the Olympus BO1.1 turbojet. (November 2006)

[14] Wikimedia Commons [Online], Available:

https://upload.wikimedia.org/wikipedia/commons/4/4c/Jet_engine.svg

[15] Mr. Bouhaf, "Course of turbomachine M2 ELM"

[16] Jingzhou Zhang. Shenghang Zhang. Chunhua Wang. Xiaoming Tan, "Recent advances in film cooling enhancement: a review"

[17] Yahya, SM, "Chapter 10: High temperature (cooled) turbine stages". *Turbines, compressor and fans (4th ed.)*. New delhi: Tata McGraw Hill Education private limited. (2011). ISBN 978-0-07-070702-3

[18] Acharya, Sumanta; Kanani, Yousef (1 January 2017), Sparrow, Ephraim M.; Abraham, John P.; Gorman, John M. (eds.), "Chapter Three - Advances in Film Cooling Heat Transfer", *Advances in Heat Transfer*, Elsevier, vol. 49, p. 91–156, doi:10.1016/bs.aiht.2017.10.001, retrieved (30 August 2019)

[19] Flack, Ronald D, "Chapter 8: Axial Flow Turbines". *Fundamentals of Jet Propulsion with Applications. Cambridge Aerospace Series*" New York, NY: Cambridge University (2005). ISBN 978-0-521-81983-1

[20] Wikimedia Commons [Online],

Available: https://en.wikipedia.org/wiki/File:Cooling_by_Convection.jpg

[21] Dr.David G. Bogard "Airfoil Film Cooling". *Mechanical Engineering Department University of Texas at Austin*

[22] baskaran, "Bearing chamber cooling, Development of high pressure turbine blade cooling, high pressure nozzle guide vane construction and cooling, Accessory cooling"
[23] Yunus A Çengel, "Heat transfet", (1997).

[24] Wahab, M.A. "The Mechanics of Adhesives in Composite and Metal Joints: Finite Element Analysis with Ansys". (2014).

[25] Khaled Al-Farhany, "Heat Transfer Simulation of Gas Turbine Blade with Film Cooling", Head of the Department of Mechanical Engineering University of Al-Qadisiyah [Iraq]